Brain Research Unit, O.V. Lounasmaa Laboratory

Advances in modeling and characterization of human neuromagnetic oscillations

Pavan Ramkumar

Aalto University

DOCTORAL DISSERTATIONS

Aalto University publication series
DOCTORAL DISSERTATIONS 56/2012

Advances in modeling and characterization of human neuromagnetic oscillations

Pavan Ramkumar

Doctoral dissertation for the degree of Doctor of Science in Technology to be presented with due permission of the School of Science for public examination and debate in Auditorium U142, Otakaari 1G, at the Aalto University School of Science (Espoo, Finland) on the 7th of May 2012 at 12 noon.

Aalto University
School of Science
O.V. Lounasmaa Laboratory
Brain Research Unit

Supervisors
Prof. Samuel Kaski
Department of Information and Computer Science
School of Science, Aalto University
Finland

Instructors
Acad. Prof. Riitta Hari
Brain Research Unit, O.V. Lounasmaa Laboratory
School of Science, Aalto University
Finland

Prof. Aapo Hyvärinen
Department of Computer Science and
Department of Mathematics and Statistics
University of Helsinki
Finland

Preliminary examiners
Dr. Jussi Tohka
Department of Signal Processing
Tampere University of Technology
Finland

Prof. Matti Hämäläinen
Department of Radiology
Harvard Medical School
USA

Opponents
Prof. Richard Leahy
Department of Electrical Engineering
Viterbi School of Engineering
University of Southern California
USA

Aalto University publication series
DOCTORAL DISSERTATIONS 56/2012

ISBN 978-952-60-4615-0 (printed)
ISBN 978-952-60-4616-7 (pdf)
ISSN-L 1799-4934
ISSN 1799-4934 (printed)
ISSN 1799-4942 (pdf)

Unigrafia Oy
Helsinki 2012

Finland

The dissertation can be read at http://lib.tkk.fi/Diss/

441 697
Printed matter

Aalto University

Abstract

Aalto University, P.O. Box 11000, FI-00076 Aalto www.aalto.fi

Author
Pavan Ramkumar

Name of the doctoral dissertation
Advances in modeling and characterization of human neuromagnetic oscillations

Publisher School of Science

Unit O.V. Lounasmaa Laboratory

Series Aalto University publication series DOCTORAL DISSERTATIONS 56/2012

Field of research Information and Computer Science

Manuscript submitted 20 February 2012 **Manuscript revised** 16 April 2012

Date of the defence 7 May 2012 **Language** English

☐ **Monograph** ☒ **Article dissertation (summary + original articles)**

Abstract

Intracranial electrophysiological measurements as well as electromagnetic recordings from the scalp have shown that oscillatory activity in the human brain plays an important role in sensory and cognitive processing. Communication between distant brain regions seems to be mediated by oscillatory coherence and synchrony. Our brain is both reactive and reflexive: it reacts to changes in the external environment, but it is also influenced by its past and present internal state. On the one hand, task-related or induced modulations of oscillatory activity provide an important marker for cortical excitability and information processing of the reactive brain. On the other hand, spontaneous oscillatory dynamics subserves information processing of the reflexive brain.

In this thesis, methods were developed to model and characterize task-related oscillatory changes, as well as spontaneous oscillatory activity measured using magnetoencephalography (MEG). In Publication I, we developed a predictive model to capture the suppression--rebound reactivity of the ~20 Hz mu rhythm originating in the sensorimotor cortex and applied this model to locate the cortical generators of the rhythm from independent measurements. In Publications II and III, we developed temporal and spatial variants of a data-driven method to characterize spatial, temporal, and spectral aspects of spontaneous MEG oscillations. Analysis of complex-valued Fourier coefficients identified well-known rhythms, such as the parieto-occipital ~10-Hz and the rolandic ~20-Hz rhythms consistently across subjects. In Publication IV, we applied independent component analysis to time–frequency representations of cortical current estimates computed from simulated as well as resting-state and naturalistic stimulation data. Group-level analysis of Fourier envelopes also identified the ~20-Hz bilateral sensorimotor network, a subset of the default-mode network at ~8 and ~15 Hz, and lateralized temporal-lobe sources at ~8 Hz.

The methods developed here represent important advances in the modeling and characterization of the brain's oscillatory activity measured using non-invasive electrophysiological methods in healthy humans.

Keywords magnetoencephalography, oscillations, oscillatory response, mu rhythm, resting-state, naturalistic stimulation, independent component analysis, time-frequency representation

ISBN (printed) 978-952-60-4615-0 **ISBN (pdf)** 978-952-60-4616-7

ISSN-L 1799-4934 **ISSN (printed)** 1799-4934 **ISSN (pdf)** 1799-4942

Location of publisher Espoo **Location of printing** Helsinki **Year** 2012

Pages 90 **The dissertation can be read at** http://lib.tkk.fi/Diss/

Preface

This thesis is submitted in partial fulfillment of the requirements for the degree of Doctor of Science in Technology, from the Department of Information and Computer Science, School of Science, Aalto University. The thesis work was carried out in the Brain Research Unit, O.V. Lounasmaa Laboratory, Aalto University. The work was financially supported by the Finnish Graduate School of Neuroscience, the Finnish Center of Excellence in Human Systems Neuroscience (2006–2011), and the Brain2Brain European Research Council Grant.

I am incredibIy fortunate to have had two highly distinguished scientists as my supervisors and mentors, without whose faith in me, this thesis would not have been possible. I thank Prof. Riitta Hari for inviting me to the lab, for giving me a lot of academic freedom, for setting very high standards, and for always leading by example. Her compelling mastery of physiology, physics, and statistics, her clear assessment of a problem, her fair and inclusive style of leadership, her energy and effortless ability to remain inspired, and her geniune warmth and moral support have inspired me boundlessly. I also wish to thank Prof. Aapo Hyvärinen for his open and spontaneous style of teaching and guidance, his depth of knowledge, his inexhaustible store of new and brilliant ideas, and his encouragement to remain skeptical always. I am also lucky to have worked with Dr. Lauri Parkkonen who has played a significant role in the ideas developed throughout this thesis. His infinite patience and availability in practical, scientific, and philosophical matters right from the first day to the last, cannot be captued in words. He has truly been an important role model in the development of my scientific temperament and work ethic.

I would like to thank the pre-examiners of this thesis, Dr. Jussi Tohka and Prof. Matti Hämäläinen for their careful and thorough reviews. I am very grateful to the professor of my studies, Prof. Samuel

Kaski, for his encouragement and supportive attitude throughout my doctoral work. Prof. Kaski and Dr. Tohka have also played a critical role in my follow-up group.

The time spent at the O.V. Lounasmaa laboratory has been the most distinguished period of my education. The excellent workplace infrastructure, combined with the unique traditions of the lab, have been a tremendous source of motivation and mental strength. I am very grateful to the past leaders of the lab, Prof. Olli Lounasmaa and Prof. Mikko Paalanen, and the present Brain Research Unit leaders, Doc. Nina Forss, Doc. Päivi Helenius, Doc. Veikko Jousmäki, Doc. Elina Pihko, Prof. Riitta Salmelin, and Doc. Simo Vanni, for creating a wonderful environment. Special thanks are due to Ronny Schreiber and Petteri Räisänen for their readiness to help in all technical aspects. Without naming them all, I am also grateful to the past and present secretaries for helping me with my salary, travel arrangements, work permits, or taxes, with great willingness and dedication.

For their grace in putting up with me, I wish to thank my former and current office mates, M.Sc. Hannu Laaksonen, Dr. Lauri Parkkonen, M.Sc. Anne Mandel, Dr. Harri Piitulainen, Dr. Nuutti Vartiainen, Dr. Pamela Baess, Dr. Yevhen Hlushchuk, M.D. Satu Lamminmäki, Kranthi Kumar Nallamothu, and Marika Kaksonen. For excellent collaborations, I would like to thank Dr. Sanna Malinen, Dr. Nuutti Vartiainen, Dr. Miika Koskinen, Dr. Yevhen Hlushchuk, Doc. Nina Forss, Prof. Eija Kalso, Dr. Sebastian Pannasch, Mainak Jas, and Kranthi Kumar Nallamothu. I have learned from each of them, new perspectives, clever tricks, and fresh ways to stay inspired about science.

Without naming them all, I wish to thank my former and present colleagues at the lab for their friendship and mutual support, the enriching cultural and sports activities, their genuine kindness, and their uniquely Finnish humor. Thanks to them, I have been able to navigate every little workplace challenge with a smile on my face and the many delightful memories of my time in their company will remain with me always.

For keeping me sane, human, and inspired, I am very grateful to my close friends outside of work, in no particular order, Jayaprakash, Varun, Irena, László, Judit, Sebastian, Bahram, Anna, Amit, Gitika, Pardip, and Sachin. I thank the Desi Otaniemi community for their positive attitude and admirable solidarity towards all matters Indian. By creating a wel-

coming atmosphere, compassionate and intellectual in equal measure, Ian Bourgeot at the Arkadia bookshop has been a remarkable influence on my personal growth. I am also indebted to my true friend Mayur for being a tremendous source of courage and comfort during difficult times, and for walking the path of graduate school together with me, albeit across the Atlantic.

I wish to express my gratitude to Cathy, my companion, muse and confidant in these years, for being there during my lowest moments, for giving me perspective, for applauding my ordinary achievements, and for nudging me on towards greater ideals. I did not notice the many cold and dark winters rush by.

Finally, I wish to thank my parents, Ramkumar and Usha, for being my first teachers, for believing in my chosen career path, for understanding "why Finland?", and for their unconditional love.

Espoo, April 23, 2012,

Pavan Ramkumar

Contents

List of Publications

This thesis consists of an overview and of the following four publications, which are referred to in the text by their Roman numerals.

I Ramkumar P, Parkkonen L, Hari R. Oscillatory response function: Towards a parametric model of rhythmic brain activity. *Human Brain Mapping*, 31, 820–834, 2010.

II Hyvärinen A, Ramkumar P, Parkkonen L, Hari R. Independent component analysis of short-time Fourier transforms for spontaneous EEG/MEG analysis. *Neuroimage*, 49, 257–271, 2010.

III Ramkumar P, Parkkonen L, Hari R, Hyvärinen A. Characterization of neuromagnetic brain rhythms over time scales of minutes using spatial independent component analysis. *Human Brain Mapping*, In Press, 2011.

IV Ramkumar P, Parkkonen L, Hyvärinen A. Group-level spatial independent component analysis of Fourier envelopes of resting-state MEG data. *Under Revision*, 2011.

Author's Contribution

Publication I: "Oscillatory response function: Towards a parametric model of rhythmic brain activity"

My senior colleagues proposed the study of event-related modulation of neuromagnetic rhythms and a predictive model analogous to the hemodynamic response function in the fMRI literature. I developed the model using Volterra kernels with appropriate choice of basis functions. I observed that to estimate the parameters of the model, the experimental design would require multiple stimulus durations and inter-stimulus intervals. I designed the experiment and acquired the MEG data. I analyzed the data, implemented the model, and wrote the paper with input from the co-authors.

Publication II: "Independent component analysis of short-time Fourier transforms for spontaneous EEG/MEG analysis"

The ICA-based method for the analysis of resting-state MEG data was proposed, developed, and implemented by my senior authors. I acquired the MEG data, prepared the simulated dataset for Simulation 3, helped to interpret the results on human MEG data, and participated in the writing of the manuscript.

Publication III: "Characterization of neuromagnetic brain rhythms over time scales of minutes using spatial independent component analysis"

The analysis was proposed by my senior authors. I modified the experimental design from the Malinen et al. (2007) fMRI study and acquired the MEG data. Together with my senior authors, I proposed spatial and spectral sparseness as a constraint to identify functionally meaningful networks and developed and implemented the spatial Fourier-ICA algorithm. I interpreted the results in collaboration with my co-authors, and wrote the manuscript with their input.

Publication IV: "Group-level spatial independent component analysis of Fourier envelopes of resting-state MEG data"

The group-analysis was proposed by the senior author and I participated in further design of the analysis. I designed an original realistic simulated dataset, implemented the algorithm, analyzed the data, and interpreted them in collaboration with my co-authors. I wrote the manuscript as the lead author, with input from my co-authors.

1. Introduction

1.1 Motivation

Two important developments are currently taking place in systems neuroscience. First, the discovery of resting-state functional networks (Fox and Raichle, 2007) has engendered considerable interest in studying brain function in the absence of active tasks or passive perception of stimuli. Second, the study of brain function during real-world stimulation or tasks, such as watching movies (Bartels and Zeki, 2004; Hasson et al., 2004) rather than during perception of well-controlled but laboratory-created stimuli, has been increasingly emphasized.

What are the implications of this research? Studies of the resting brain can give insight to complex phenomena in cognitive science such as self-referential thinking, and in neurophysiology such as functional organization of the brain, brain metabolism or its energy budget. From studies of natural stimulation new knowledge about brain function in the real world can be obtained. An understanding of brain function in real-world like environments can help to improve the design for brain-computer interfaces.

Why are methodological advances required? Firstly, it is often unclear what the conditions of interest are in experiments with naturalistic stimulation. Hence, exploratory (as opposed to model-driven) methods are required to discover the brain regions or networks involved. Secondly, for study of complex brain functions, methods for querying distributed neural representations (as opposed to focal activation maps) of the external world are needed.

A vast majority of the resting-state and naturalistc stimulation studies have been made with functional magnetic resonance imaging (fMRI).

While fMRI provides high spatial resolution and coverage of the entire brain including subcortical areas, its temporal resolution is limited and it measures neuronal activity indirectly. For this reason, complementing such studies with magneto- and electroencephalography (MEG/ EEG) would provide tremendous value. Further, putting the two findings together may provide more insights into the basic mechanisms of neurovascular coupling. However, methodological advances for MEG/ EEG are challenging in a different manner than for fMRI. In particular, we need richer signal models to capture the time structure in addition to the spatial distribution of activation.

The studies included in this thesis address some of the above challenges in signal analysis and modeling.

1.2 Organization of the thesis

Chapter 2 of this thesis introduces electrophysiological brain rhythms, discusses their functional signifiance, emphasizes their role in oscillatory communication, and surveys some biophysical models of their dynamics. Chapter 3 reviews the concept of resting-state networks, describes some important resting-state correlations identified using fMRI, and discusses studies that have attempted to describe the electrophysiological equivalent. Furthermore, the rationale behind a move towards application of naturalistic stimuli is discussed. Chapter 4 provides a background of magnetoencephalography which is the electrophysiological technique used in this thesis. This includes a brief history of MEG, the signal generation process, the basic measurement technique, some artifact suppression methods, and a review of the inverse modeling approaches used in this thesis. Chapter 5 considers nonlinear systems identification, which is the framework used in this thesis work for modeling the stimulus-induced dynamics of brain rhythms. Chapter 6 reviews the theory of independent component analysis (ICA) and discusses its applications in neuroimaging. Particular attention is given to the use of ICA in the analysis of fMRI resting-state networks and spontaneous MEG/ EEG rhythms. Chapter 7 summarizes the objectives of the thesis. Chapter 8 summarizes the individual studies carried out in this thesis. The final Chapter 9 discusses the contributions and limitations of this thesis and offers considerations for future work.

2. Electrophysiological brain rhythms

Neural oscillations are observed throughout the central nervous system at various spatial scales ranging from single neurons, local neuronal ensembles, and concerted activity of distant ensembles, such as those in the thalamus and the cortex. Single-neuron oscillations originate from sub-threshould fluctuations in the membrane potential, or from repetitive patterns of action potentials, which in-turn produce oscillations in post-synaptic neurons. At the level of the ensemble, the conduction delays, and the balance between excitation and inhibition determine the natural frequency of these oscillations. The frequencies of neural oscillations can vary widely from < 0.1 Hz, called infra-slow fluctuations (Vanhatalo et al., 2004) to > 500 Hz, reflecting spiking activity (Baker et al., 2003).

Studies of neural oscillations attempt to describe the morphology and spatial characteristics of brain rhythms, investigate their functional significance, and discover the basic neurophysiological mechanisms of generation. The approaches include modeling techniques to understand the computational role of oscillatory ensembles, experimental manipulations to understand generative mechanisms, and statistical techniques to measure oscillatory coupling from noisy measurements. The following sections contain a brief overview of each of these areas.

2.1 Morphological and spatial characteristics

Population-level oscillatory activity is manifest in local field potentials which can be recorded with extracellular intracortical electrodes, with electrocorticography (ECoG) from the surface of the cortex, with non-invasive scalp electroencephalography (EEG), or with magentoencephalography (MEG). Given the vast variation in the spatial and spectral characteristics of oscillations, work in the early 20^{th} century focused on the

morphological description of brain rhythms and the various conditions under which they were generated and abolished.

Rhythmic activity was observed in EEG recordings by Hans Berger in 1929 much before the first MEG signals were recorded. Brain rhythms have been classified both on the basis of their frequency content and spatial distribution. Gastaut (1952) first reported the Rolandic or sensorimotor mu rhythm. As of today, the theta (4–8 Hz), the approximately sinusoidal and parieto-occipital alpha (7–13 Hz), the beta (13–30 Hz), the arch-shaped mu with 10- and 20-Hz components, and various high and low gamma-frequency bands (> 40 Hz) are routinely reported from extracranial recordings; for a review, see Niedermeyer and Da Silva (2005).

With the advent of MEG, it became possible to more easily and accurately locate the cortical generators of brain rhythms. The first report of the MEG alpha rhythm was that of Cohen (1968). The cortical sources of this rhythm cluster around the calcarine sulcus and the parieto-occipital sulcus; see Hari (2004) for a review. The first report of the MEG mu rhythm was by Tiihonen et al. (1989). The two frequency components of the mu rhythm have different topographic distributions; specifically, the 20-Hz component follows the moved body part in a somatotopic manner in the primary motor cortex, whereas the 10-Hz component does not: it originates in the hand area of the somatosensory cortex (Salmelin and Hari, 1994; Salmelin et al., 1995). Owing to its origin at the motor cortex, the coherence between the cortical 20-Hz component and electromygraphic signals from the body has been used as a reliable tool to map the motor cortex for presurgical planning (Mäkelä et al., 2001). MEG theta (3–7 Hz) oscillations have been reported in frontal areas (Sasaki et al., 1994) and gamma oscillations (30–70 Hz) in the visual cortex (Hoogenboom et al., 2006). Occasionally, the tau rhythm (8–10 Hz) can be observed in the auditory cortex (Tiihonen et al., 1991).

2.2 Functional significance

While many rhythms occur spontaneously in the brain (i.e. in the absence of task or stimulus), their amplitudes are modulated by external events. Different features of the rhythm may serve as markers for understanding their functional involvement in stimulus processing and tasks. In particular, the amplitude (also, baseline power or baseline level) of the rhythm may be suppressed or enhanced depending on the cortical region where

the oscillations are generated. The mechanism behind macroscopic suppression or enhancement is not known conclusively, since a larger signal amplitude can either be explained by an increase in synchronization or the recruitment of a larger number of neurons. The change in amplitude of a rhythm may be directly evoked by external stimulation, and therefore be strictly phase-locked, or induced in an indirect manner and therefore be time-locked but not phase-locked. The frequency of the rhythm may also be modulated by external events.

2.2.1 Sensory and cognitive function

The parieto-occipital alpha rhythm is suppressed during visual input, visual memory and imagery tasks and enhanced when the subject is relaxed with eyes closed, or during mental arithmetic. The amplitude of the alpha rhythm has thus been suggested to represent the level of cortical inhibition; see Klimesch (1996) for a review. However, more recent studies have suggested that 10-Hz oscillations do not merely reflect cortical inhibition but rather have very specific functional roles. For instance, 10-Hz ampitude enhancement in the parietal and central regions correlates with working memory load (Jensen et al., 2002).

The rolandic mu rhythm is suppressed during motor action, as well as during electrical and tactile stimulation. As reviewed by Hari and Salmelin (1997), both the 10-Hz and the 20-Hz components are suppressed below the baseline level during stimulation, exceed the baseline level (or, rebound) when the stimulation ends, and subsequently return to baseline. The 20-Hz component rebounds earlier and faster than the 10-Hz component. The mu rhythm has been used to probe the state of the sensorimotor system under various perceptual states; for instance, mu activity is clearly suppressed during motor imagery (Schnitzler et al., 1997) and observation of motor action (Hari et al., 1998; Caetano et al., 2007). This reactivity of the rhythm resembles the reactivity during real motor actions.

Palva and Palva (2007) note that unlike the ambiguity inherent in the mechanistic interpretation of amplitude, phase synchronization between distant cortical areas, although difficult to estimate robustly, is at least roughly indicative of synchronized spike-timing. Phase-locking has been reported in MEG data between the contralateral primary and ipsilateral secondary somatosensory cortices after medial nerve stimulation (Simões et al., 2003). Studies of phase synchrony during cognitive tasks

are relatively recent. For example, Palva et al. (2005b) discovered that 10-Hz activity in the frontal and parietal cortices selectively phase-locked to consciously perceived somatosensory stimuli.

Spontaneous cortical rhythms provide important spatial and temporal constraints on mechanisms of speech perception and production. For example, Giraud et al. (2007) showed the hemispheric lateralization of spontaneous gamma and theta rhythms. In particular, they reported from simultaneous EEG–fMRI measurements during rest, that gamma power correlated better with the left auditory cortex BOLD signals whereas theta fluctuations correlated better with the right auditory cortex.

2.2.2 Functional connectivity

It has been proposed that complex cognitive function arises from a balance between functional specialization of relatively independent cortical areas and coordination among several specalized areas (Bressler and Kelso, 2001). Oscillations have been thought to mediate inter-regional communication in the cortex or between the cortex and subcortical areas. Fries (2005) postulated that coherently oscillating neuronal groups are temporally aligned for communication because their inputs and outputs are open simultaneously, and that dynamically-deployed coherent networks consitute the fundamental mechanism of cortical computation (Fries, 2009). Although the mechanistic details of interaction between brain areas are not known, multiple candidates have been postulated and observed empirically, including amplitude–amplitude coupling, spectral coherence (Gross et al., 2001), within-frequency phase synchronization (Simões et al., 2003), phase-amplitude coupling (Canolty et al., 2006; van der Meij et al., 2012), and cross-frequency phase synchronization (Palva et al., 2005a). Decreased amplitude is also accompanied by increased coherence or phase synchrony; see for instance Kujala et al. (2012). Modeling studies have suggested that such a mechanism enables enhanced information transfer between brain regions (Buehlmann and Deco, 2010).

Aberrant inter-regional oscillatory coupling can serve a marker of neuropsychiatric or neurodegenerative disorders. For instance, enhanced beta oscillations in the subthalamic nucleus and the cortex have been reported in Parkinson's disease (Mallet et al., 2008). Likewise, abnormal synchrony between brain regions has been reported in schizophrenia (Uhlhaas et al., 2008). More recently, abnormal entrainment of auditory-cortex oscillations in the 25–35 Hz range has been found to correlate with

phonological deficits in dyslexia (Lehongre et al., 2011).

Precentral 20-Hz and postcentral 10-Hz EEG rhythms have been reported to inversely correlate with the blood oxygen level dependent (BOLD) fMRI signal (Moosmann et al., 2003). Some correlations between different EEG rhythms and resting state networks of BOLD activity have also been reported (Mantini et al., 2007). Thus, amplitude-amplitude oscillatory coupling is also a prime candidate for the neural mechanisms underlying fMRI resting-state networks (see Chapter 3).

2.3 Modeling of brain rhythms

2.3.1 Biophysical models of rhythm generation

A popular model of spontaneous alpha rhythms is the neural mass model (Jansen and Rit, 1995) based on earlier work by Lopes da Silva et al. (1974). This model comprises a system of three interacting neural populations: pyramidal neurons, excitatory interneurons, and inhibitory interneurons. The pyramidal neuron population receives direct external input (representing the sum total of thalamic and long distance cortico-cortical input) as well excitatory and inhibitory inputs from the respective interneuron populations. Each interneuron population in turn receives excitatory input from the pyramidal neurons. The synaptic inputs to all the populations are modeled by scaling the average presynaptic firing rate by a constant, which represents synaptic gain. The transformation of this synaptic input into postsynaptic potentials is modeled by a linear convolution, with different impulse response functions for excitatory and inhibitory synapses. For each population, the net postsynaptic potential is transformed to an average firing rate by a sigmoid function. With this model, Jansen and Rit (1995) showed that by feeding uniformly distributed white noise as external input to the pyramidal neurons, the average postsynaptic potential of the pyramidal neuron population resembled the temporal dynamics of the alpha rhythm observed in EEG recordings.

A variant of the neural mass model has been proposed by David and Friston (2003) as a building block for dynamic causal modeling, a framework for discovering causal relationships between different neuronal sources of activity. More recently, Jones et al. (2009) proposed a bio-

physically realistic laminar network model of the primary somatosensory cortex (SI) which predicts evoked MEG response to tactile stimulation as a function of the pre-stimulus mu rhythm level. Based on simulations, they suggested that the 10- and 20-Hz components of the mu rhythm may be produced by feed-forward and feedback drive, respectively, to SI at 10 Hz. In a later study by Ziegler et al. (2010), this model was used to account for differences in pre-stimulus 10-Hz power by simulating stronger feed-forward and feedback inputs.

2.3.2 Models of oscillatory communication

Purely mathematical models of brain rhythms which simulate ensembles of oscillators intend to account for the different forms of oscillatory coupling with the intention of understanding what factors give rise to observed oscillatory dynamics in an ensemble (Pikovsky and Rosenblum, 2007). These models typically do not account for any biophysical constraints in which neurons live. In contrast, biophysical models attempt to model real neural networks by taking conduction delays, neuronal geometries, as well as excitatory and inhibitory connections into account.

The mathematical models have been able to propose and clarify the potential computations that can be carried out by an ensemble of oscillators exhibiting a particular regime of synchrony (Bressler and Kelso, 2001; Ermentrout and Chow, 2002). These proposals in turn constrain speculations about functional significance and inform new experiments. By including realistic constraints, biophysical models of long-range functional connectivity help to understand the role of coupling, delay and noise in resting-state fluctuations. By simulating noise-driven oscillators to interact with realistic delays based on the lengths of primate cortico-cortical pathways, Deco et al. (2009) showed the emergence of two sets of 40-Hz oscillators which were anticorrelated at < 0.1 Hz.

Besides modeling work, it is also important to recognize that experimental work together with robust statistical measures of coupling, such as dynamics imaging of coherent sources (Gross et al., 2001), phase-locking value, and phase-locking statistics, as well as statistical causal measures of directional influence such as Granger causality (Granger, 1969), can inform and constrain mathematical models of coupling phenomena.

While it is important to acknowledge the contributions of modeling work and statistical methods, the focus of this thesis was more straight-

forward: we aspired simply to provide accurate descriptions of spatiotemporal and spectral and distributions of cortical rhythmic activity.

3. Resting-state networks and naturalistic stimulation

3.1 Resting-state networks

It has been known for the past 50 years that the metabolic rate of the brain during active sensorimotor or cognitive tasks is only less than 5% higher than the metabolic rate during quiet rest. Further, 60–80% of the brain's energy budget during rest is involved in neuronal signaling (Raichle and Mintun, 2006). Until recently, however, the characteristics of intrinsic brain activity were largely unknown.

Resting-state networks (RSNs) refer to the recently discovered phenomenon of spatial correlations in brain activity during rest, i.e. when the subject is not engaged in executing any specific task or perceiving any specific external stimuli; for a review see Fox and Raichle (2007). Biswal et al. (1995) first observed correlations between the left and right sensorimotor cortices in resting fMRI fluctuations. Subsequently, Shulman et al. (1997) conducted a comprehensive meta-analysis of positron emission tomography (PET) studies, which revealed a task-related increase in blood flow in some brain regions, and a corresponding task-related decrease in others, across a wide variety of visual and language tasks. The regions showing task-related decreases were thought to mediate a default mode of brain function and this hypothesis was explicitly confirmed using seed-based resting-state correlations of fMRI data (Greicius, 2003). Fox et al. (2005) reported task-positive and task-negative brain regions which were enhanced and suppressed respectively during task performance, with respect to a baseline level of BOLD activity. Task-positive regions overlapped with regions reported to be involved in attention and executive control, whereas the task-negative regions were together named the default mode network (DMN). Since then, using seed-based correlations as

well as independent component analysis (see Section 6.2), a number of other resting-state networks have been identified including the dorsal attention networks, the auditory network, the cerebellar network, the executive control network, and the visual network. (Damoiseaux et al., 2006; Fox and Raichle, 2007; Smith et al., 2009).

How do the functional RSNs relate to the anatomical connections of the brain? Honey et al. (2009) showed that anatomical connectivity estimated using diffusion tensor imaging could only partially explain the variance of functional connectivity; interregional distance and indirect connections could explain only part of the remaining variance.

What, if any, is the functional significance of RSNs? One possibility is that since RSNs were primarily observed in PET and fMRI, they could be related to vascular phenomena with no neural correlates. However, this proposal has come to be contested by direct electrophysiological observations of resting-state correlations (de Pasquale et al., 2010; Brookes et al., 2011). The DMN has been suggested to be involved in stimulus-independent thought or self-referential processing (Mason et al., 2007). However, mediation of conscious mental tasks cannot be its only role since DMN activity has been shown to persist under light sedation and early stages of sleep (Larson-Prior et al., 2009; Greicius et al., 2008). Although its functional role is not clearly established, the DMN has served as an excellent marker for human brain development (Fair et al., 2008), aging (Andrews-Hanna et al., 2007), and Alzheimer's disease (Buckner et al., 2005), and other neuropsychiatric disorders (Greicius, 2008).

Electrophysiological methods, owing to their direct measure of neuronal activity, offer a complementary view of RSNs. The electrophysiological correlates of the RSNs characterized using fMRI are an area of active research. The best electrophysiological correlates of the BOLD signal seem to be local field potentials (LFPs) (Logothetis et al., 2001). Different frequency bands of the LFP predict the BOLD signal latency and amplitude to different extents (Magri et al., 2012). Electrocorticography (ECoG), scalp EEG, and MEG essentially reflect summations of large populations of LFPs. Although a rich literature has described the characteristics of spontaneous electrical oscillations in the brain (see Chapter 2), neural evidence for long-range resting-state correlations is only beginning to surface.

Given the slow nature of intrinsic hemodynamic fluctuations, one candidate neural mechanism is sought in the correlations between band-

limited power fluctuations or amplitude envelopes of spontaneous oscillations. The evidence for this candidate mechanism comes from invasive and non-invasive studies in animals and humans. I briefly summarize these findings below.

Lu et al. (2007) demonstrated electrophysiological correlations in delta band power between bilateral primary sensorimotor cortices in anesthetized mice. Leopold et al. (2003) found gamma band power correlations at < 0.1 Hz in the monkey visual cortex. Nir et al. (2008) studied firing-rate modulations and gamma power modulations of intracranial signals from auditory cortices of humans. They found robust inter-hemispheric correlations of both firing-rate modulations and gamma power at frequencies < 0.1 Hz during wakeful rest, rapid-eye-movement (REM) sleep, and stage 2 sleep. He et al. (2008) reported a similar correlation structure between slow cortical LFPs (0.01–0.1 Hz) and BOLD fMRI during wakefulness, slow-wave sleep and REM sleep. Studies examining the relationship between spontaneous MEG/ EEG oscillations and BOLD RSNs using simultaneous EEG and fMRI or simultaneous EEG and near infrared spectroscopy (NIRS) have found that the power of the alpha rhythm is inversely correlated with the fMRI signal in the occipital areas but positively correlated with the thalamus and insula (Goldman et al., 2002; Moosmann et al., 2003). Laufs et al. (2003) reported mainly negative correlations between the occipital alpha power and fMRI signals in a fronto-parietal network, but mainly positive correlations between occipital beta power and in the temporo-parietal junction and the cingulate cortex. However, Mantini et al. (2007) found mainly positive correlations between BOLD signals and average EEG power in different frequency bands. Although the details about the contribution of individual frequency bands towards the BOLD signal do not entirely agree, and new data continue to emerge (Magri et al., 2012), the above studies taken together support band-limited power correlations as the electrophysiological mechanism underlying RSNs.

More recently, de Pasquale et al. (2010) reported non-invasive seed-based correlations in the default mode network using MEG. Brookes et al. (2011) reported robust MEG RSNs at the group level using temporal independent component analysis on MEG data in source space.

3.2 Advantages and challenges of naturalistic stimulation

One of the goals of systems neuroscience is to understand how various brain systems encode, represent, and generalize information about the natural environment. Beginning with the discoveries of Hubel and Wiesel (1963), we have gained a tremendous amount of knowledge about the detailed neuronal representations of very specific enviromental features using elementary stimuli, such as oriented edges, gratings, or pure tones, which can be readily parametrized. White-noise stimuli, whose properties are well known for learning transfer functions of nonlinear systems, have also been effective tools to characeterize single neurons (Marmarelis and McCann, 1973). Therefore, the role of these elementary stimuli in investigations of neural systems has been firmly established.

In recent years, functional brain imaging studies as well as single-unit studies in humans have revealed that the brain contains dedicated systems, circuits and even single neurons tuned to a narrow range of natural stimuli such as faces (Haxby et al., 1996; Kanwisher et al., 1997), scenes (Epstein and Kanwisher, 1998), or even a particular face (Quiroga et al., 2005). These systems, circuits, and neurons are very difficult to drive using elementary stimuli alone (Felsen and Dan, 2005). Although this shortcoming has been circumvented to some extent by using a sparse basis set for generating pseudo-random stimuli, the properties of the systems characterized are biased by the choice of the basis. This is a limitation that can be overcome with naturalistic stimuli, defined roughly as stimuli representative of the natural environment.

However, naturalistic stimuli present at least three methodological challenges. First, we do not have a well-defined response model for complex stimuli such as videos or continuous speech. As a result, it is difficult to build predictive models of brain responses. This constraint requires exploratory, data-driven methods to effectively separate the various systems involved. Second, these stimuli are difficult to present multiple times and therefore novel methods which enhance the signal-to-noise ratio or contrast-to-noise ratio from single responses need to be developed. Third, we need computational methods to design and parametrically manipulate the naturalistic stimuli.

The first steps towards using naturalistic stimuli in fMRI have already been taken, with suprising results. Bartels and Zeki (2004) first showed that naturalistic stimuli can activate a large number of neural

systems at the same time. Hasson et al. (2004) demonstrated the consistency of responses to natural stimuli by reporting high degree of inter-subject correlations during movie viewing, and later on attributing this high correlation to encoding of episodic memory (Hasson et al., 2008a). Golland et al. (2007) characterized extrinsic networks, reliably driven by naturalistic audiovisual stimuli, as well as intrinsic networks whose activity was dissociated from the external stimulation. Malinen et al. (2007) showed using independent component analysis that systems related to processing of naturalistic auditory, visual, and tactile stimulation can be separated reliably. Hasson et al. (2008b) used silent films played forward, in reverse or piecewise-scrambled to elucidate a temporal hierarchy of visual information processing in the cortex. These studies illustrate the unique possiblities afforded by naturalistic stimuli to characterize neural systems and the potential for data-driven methods to enable such characterization.

4. Magnetoencephalography

This chapter presents a brief introduction to MEG, the main experimental technique used in this thesis, followed by a short background of the principles of signal generation, data acquisition, and analysis. This chapter refers very often to the classic reviews by Hämäläinen et al. (1993) and Hari (2004), and a recent historical account by Hari and Salmelin (2012).

4.1 History

Magnetoencephalography (MEG) is a technique to measure magnetic fields associated with neural electrical currents. As a non-invasive brain imaging technique, MEG offers an excellent temporal resolution (less than a millisecond) and a good spatial resolution (in the range of 5–30 millimeters, depending on source configuration, orientation and location).

The first MEG measurements were conducted in the late 1960s with an induction-coil magnetometer (Cohen, 1968). However, a high enough signal-to-noise ratio for real-time recordings was achieved with a magnetometer utilizing the superconducting quantum interference device (SQUID) as a sensor (Cohen, 1972).

Early EEG studies mostly focused on characterizing the morphological properties of spontaneous activity and correlating these with mental and disease states, as outlined in Chapter 2. It was only in the 1960s with the advent of laboratory computers that signal averaging became feasible (Hari and Salmelin, 2012). By quantifying response latencies and amplitudes, averaged evoked responses allowed investigators to assess the integrity of various functional pathways.

Owing to advances in inverse modeling (Section 4.5), it became possible from the late 1970s to non-invasively locate cortical generators of various responses evoked by visual, auditory and somatosensory stimua-

tion. Averaging was also applied to the envelopes of ongoing oscillations and it became possible to quantify their modulations as a function of stimulation, as well as to pinpoint their cortical sources. Thanks to parallel advances in multichannel MEG instrumentation, these strengths of MEG led to clinical applications in locating the foci of epileptic seizures as well as in presurgical mapping of eloquent brain areas by the 1990s (Stefan et al., 2003; Papanicolaou et al., 2004). MEG applications in cognitive neuroscience include primary sensory cortical function, attention, action-observation, and language production and perception.

In the past decade, MEG studies have begun to move beyond the quantification of evoked-responses and the emphasis on accurate location of brain activation towards studying cortico-cortical functional connectivity. Owing to the recent interest in spontaneous brain activity emerging from other imaging domains such as PET and fMRI (see Chapter 3), it has once again become popular to study oscillatory activity and spontaneous fluctuations using electrophysiological techniques, and MEG is often seen as the primary imaging method in such investigations. In this sense, the historical progress of MEG has taken place in a direction opposite to that of EEG, with early investigations dominated by evoked reponse studies, and current and future investigations likely to be dominated by studies of spontaneous activity. However, the hope is that with advanced inverse modeling techniques and nuanced statistical measures of functional connectivity, we can move beyond morphological descriptions and associations between activation and cognitive states, towards quantitative descriptions and predictive models of brain function.

4.2 Signal generation

Synchronous postsynaptic currents in the apical dendrites of tens of thousands of neurons give rise to a weak magnetic field which is detectable outside the head. It is believed that the bulk of the extracranial fields is due to postsynaptic currents for two reasons. Firstly, the pyramidal neurons are oriented parallel to each other, and the postsynaptic potentials are long-lasting enough (compared with action potentials) to allow for temporal summation (Hari, 1990; Okada et al., 1997). Secondly, the magnetic field pattern due to a postsynaptic current is dipolar in nature, i.e. the field strength falls off as $1/r^2$. In comparison, the quadrupolar field due to an action potential falls off as $1/r^3$ (Hämäläinen et al., 1993).

Ampere's law with Maxwell's correction states that electric currents and changing electric fields generate magnetic fields:

$$\nabla \times \mathbf{B} = \mu\mathbf{J} + \mu\epsilon\frac{\partial \mathbf{E}}{\partial t} \ , \tag{4.1}$$

where $\mathbf{B}$ is the magnetic field, $\mathbf{J}$ is the total current density, $\mathbf{E}$ is the electric field, and μ and ϵ are the magnetic permeability and the electric permittivity of the medium, respectively.

The current density $\mathbf{J}$ in Eq. 4.1 represents the sum of primary currents $\mathbf{J_p}$ and volume currents $\mathbf{J_v}$. Primary currents for MEG flow mainly inside the neuron as a direct consequence of the electric potential set up at the synapse. Volume currents flowing in the conducting medium outside the neurons close the current loop. The term $\mu\epsilon\frac{\partial \mathbf{E}}{\partial t}$ may be neglected because time derivatives are insignificant at the maximum frequency of interest (about 100 Hz) for the spatial scale of the human head (Hämäläinen et al., 1993). This is known as the quasistatic approximation.

If the head is approximated as a homogeneous spherical conductor, then the net effect due to volume currents can be taken into account analytically. However, for more realistic geometries and conductor models, volume currents must be taken into account numerically (see for e.g. Tanzer (2006)). In addition, in a spherically symmetric conductor, radially oriented primary currents do not produce any magnetic field outside the conductor, see Fig. 4.1.

The decrease of field strength with source depth limits the depth resolution offered by MEG. This phenomenon is both due to increasing measurement distance and the spherical head shape, implying that the MEG signal is predisposed to superficial currents. However, since pyramidal neurons are oriented perpendicular to the cortical sheet, MEG detects sources from the cortical sulci better than EEG, whereas EEG is better at detecting sources from the convexial cortex, as well as from the depth of the brain. For these reasons, MEG and EEG complement each other.

4.3 Measurement

The magnetic field of the brain is of the order of 10^{-14}–10^{-13} T for evoked fields, and of the order of 10^{-12} T for prominent alpha oscillations, about 8–10 orders of magnitude below the earth's magnetic field and 7 orders of magnitude below the field generated by typical laboratory appliances. Hence, the instrumentation required to detect these fields must be highly

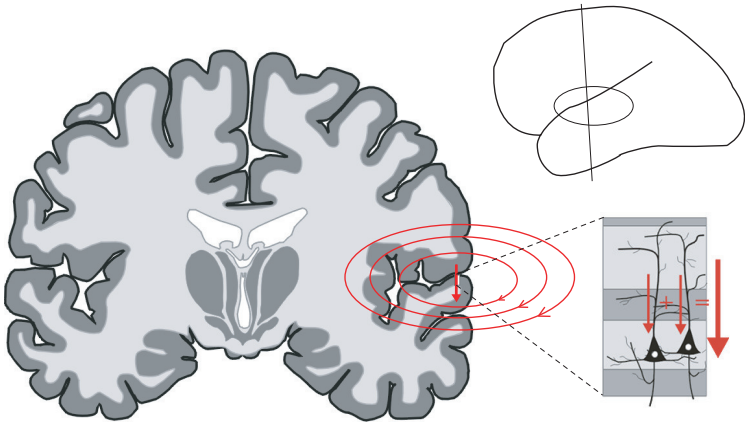

Figure 4.1. MEG is maximally sensitive to primary currents which are tangential to the surface of the head. This figure shows a coronal section of the brain with a current source in the lateral fissure. The primary current that produces an extracranially measurable magnetic field, shown schematically as a red arrow, is the result of temporal and spatial summation of currents over a cortical area of approximately 40–200 mm^2 (Hari, 2004). The spatial summation is possible due to parallely-oriented pyramidal neurons. Image courtesy of Lauri Parkkonen.

sensitive.

Although the first MEG signal was detected by an induction coil magnetometer (Cohen, 1968), with the invention of the Josephson junction it became possible to measure biomagnetic fields using a superconducting quantum interference device (SQUID) magnetometer (Zimmerman et al., 1970; Cohen, 1972). Modern MEG sensors are based on SQUIDs whose white-noise levels can be as low as $1 \mathrm{fT}/\sqrt{\mathrm{Hz}}$. Liquid helium is used to keep the SQUIDs superconducting at a temperature of about 4 K. Such a temperature difference requires good isolation of the sensor element from the head surface, limiting the measurement distance. With the deployment of whole-scalp MEG systems (Ahonen et al., 1993) it became possible to record magnetic fields from all over the brain surface. Modern MEG systems consist of more than 300 sensors whose orientations are optimized to maximize the information provided by the acquired signals (Nenonen et al., 2004).

The data presented in this thesis were acquired using a Vectorview system (Elekta Neuromag Oy, Helsinki, Finland) which comprises 102 sensor elements, each containing a magnetometer and two orthogonal planar gradiometers. Magnetometers measure the magnetic field component normal to the head, while the planar gradiometers measure the spatial gradient of the field component in a plane tangential to the head surface

at the site of each sensor element. To minimize external interference, the MEG system is operated in a magnetically shielded room. The shielding is provided by layers of mu-metal and aluminum. In our three-layer shielded room (Cohen et al., 2002), the low frequencies (< 10 Hz) are attenuated by a factor of 10^3 to 10^4, while at higher frequencies the shielding factor is at least 10^5.

4.4 Artifact suppression

MEG recordings may be corrupted by a number of artifacts originating from physiological sources such as eye-blinks, saccades, head movements, muscle artifacts, respiration and the electrical signal from the heartbeat, as well as non-physiological sources such as line noise, slow drifts in the external magnetic field, etc.

The most rudimentary approaches towards artifact removal involve discarding channels or measurement epochs with clearly artifactual patterns, and linear filtering to limit slow drifts, line noise, or high frequency artifacts. However, this approach is not feasible if the brain signals and artifacts are in the same frequency range.

Signal-space projection (SSP) is a method to separate MEG signals from various non-physiological sources of noise (Uusitalo and Ilmoniemi, 1997). The approach relies on linearly projecting the measured signal into a signal subspace (the signal-space). To estimate the signal subspace, a typical approach is to subtract the artifactual subspace from identity. The artifactual subspace in turn is identified by performing a singular value decomposition on measurements obtained in the presence of external interference.

Data-driven methods such as independent component analysis are also useful to separate temporally uncorrelated or independent artifactual sources from sources of interest, see e.g., Vigário (1997).

Another robust method to separate artifacts from brain signals that has been applied in this thesis, is based on separating the signal contributions from inside and outside the head (Taulu and Kajola, 2005; Taulu and Simola, 2006). This method is known as signal-space separation. The net magnetic field at each sensor contains both the signal of interest arising from inside the head and the interference arising from contaminating sources outside the helmet-shaped sensory array. Because the sensors are located in a source-free volume outside the volume of interest, the

magnetic field can be expressed in the sensor domain as a gradient of a magnetic scalar potential. Since the divergence of the magnetic field vanishes, this scalar potential is a harmonic function. The signal space can be expanded as the summation of two subspaces, known as the multipole expansion.

In the former subspace, the field is generated by sources within the volume of interest (the head). By contrast, in the latter subspace, the contribution to the field comes from the volume of no interest (outside the sensor-array). After the coefficients corresponding to the two subspaces have been estimated, the latter subspace, which represents only the unwanted external interference, is discarded.

It can be shown that the contributions to the signal from within and outside the sensor array are temporally uncorrelated for a suitable truncation length of the multipole expansion. However, if the artifacts arise from inside the sensor volume, such as due to head movements, they leak into both subspaces. By removing the temporal statistical correlations between these subspaces, interference arising from within the sensor array can be further suppressed; this approach is called the temporal signal-space separation method (tSSS); (Taulu and Simola, 2006).

4.5 Inverse modeling

The problem of inferring the neuronal primary current distribution that gives rise to the measured extracranial fields is known as the neuromagnetic inverse problem. It was already shown by Helmholtz in the 19^{th} century that a current distribution inside a conductor cannot be uniquely reconstructed from the electromagnetic fields outside it (Hämäläinen et al., 1993) without making certain assumptions about the distribution.

The equivalent current dipole (ECD) model is the most commonly applied source modeling technique for MEG. In this approach, one assumes that the actual source distribution can be faithfully represented by a small number of current dipoles. The dipole parameters (position, orientation and strength) are then estimated by minimizing the least-squares error between the measured data and those predicted by the model. Each current dipole is described by three parameters for position and three parameters for the strengths of the orthogonal components of the dipole vector. Since radial currents do not produce any magnetic field in the sphere model, one of the dipole components is constrained to be zero if spherical

symmetry is assumed and only the two tangential components remain.

In a typical whole-scalp system, measurements from more than 100 channels are available, and the inverse problem is thus overdetermined, i.e., we have more observations than unknowns. Although ECD modeling has been highly effective to locate neural generators of evoked responses when a reasonable guess of the active sources is available a priori, it is not straightforward to select a model structure when a large number of temporally overlapping sources and noise are present simultaneously. An even more significant problem is that a fully automated reliable optimization procedure does not exist in the case of multiple dipoles.

By contrast, in distributed source models, a grid of source points is defined on the brain surface or volume, known as the source space. Each source point typically contains three orthogonal current dipoles whose strengths are estimated from the measured data. Due to the large number of source points, the inverse problem is underdetermined and additional constraints are required to render the problem unique. The minimum-norm models (Hämäläinen and Ilmoniemi, 1994; Uutela et al., 1999) seek a current distribution that explains the observed field, subject to the constraint that the norm of the entire primary source current is as low as possible. The most popular norm is the L_2-norm, and this solution is commonly called the minimum norm estimate (MNE). The observed field

$$\mathbf{B} = \mathbf{L}\mathbf{J} + \mathbf{n} \tag{4.2}$$

where $\mathbf{J}$ is the vector of current source strengths at each location and orientation, $\mathbf{L}$ is the linear, discretized forward operator, or lead field matrix, which analytically gives the value of the field at each sensor due to a unit dipole at each source location, and n is the noise vector. The minimum-norm estimate is obtained as the solution of the minimization problem

$$\hat{\mathbf{J}} = \min_{\mathbf{J}} \|\mathbf{B} - \mathbf{L}\mathbf{J}\|^2 + \lambda^2 \|\mathbf{J}\|^2 \tag{4.3}$$

where λ is the regularization parameter which weights the relative importance of obtaining a good fit to the data and minimizing the total source current. If λ is large, the estimated current distribution will have a small amplitude and will be spatially smooth. With decreasing λ, the current distribution becomes stronger and shows more spatial variations. Placing more emphasis on the first term in Eq. 4.3 thus introduces these variations to explain the measurements accurately. The implicit assumptions in this model are that (1) the noise level is the same in all channels,

(2) noise is uncorrelated across sensors, (3) sources are equally likely to be of the same strength, and (4) each source is uncorrelated from all others.

We can relax assumptions (1) and (2) if an estimate of the noise-covariance matrix is available. Such an estimate can be obtained from data with no brain signal of interest, e.g., from a recording without a subject present. With this information, it is possible to capture noise levels in the sensors and account for noise being correlated across channels. Similarly, with a realistic source covariance matrix, assumptions (3) and (4) can be relaxed. Through this matrix, insights from fMRI activations into possibly active source areas, anatomical constraints (Dale and Sereno, 1993), sensitivity constraints such as such as the depth bias of MEG (Ioannides et al., 1990; Lin et al., 2006), or spatial correlation of neighboring sources (Pascual-Marqui et al., 1994) can be incorporated. If $\mathbf{C}$ is the noise covariance matrix and $\mathbf{R}$ is the source covariance matrix, the weighted cost function for the computation of the MNE can be re-written as

$$\hat{\mathbf{J}} = \min_{\mathbf{J}} (\mathbf{B} - \mathbf{L}\mathbf{J})^{\mathrm{T}} \mathbf{C}^{-1} (\mathbf{B} - \mathbf{L}\mathbf{J}) + \lambda^2 \mathbf{J}^{\mathrm{T}} \mathbf{R}^{-1} \mathbf{J}^{\mathrm{T}}. \tag{4.4}$$

The solution of this problem is $\mathbf{J} = \mathbf{M}\mathbf{B}$, where $\mathbf{M}$ is the closed-form linear inverse operator is given by

$$\mathbf{M} = \mathbf{R}\mathbf{L}^{\mathrm{T}} (\mathbf{L}\mathbf{R}\mathbf{L}^{\mathrm{T}} + \lambda^2 \mathbf{C})^{-1}. \tag{4.5}$$

The inverse solution is then visualized by plotting the estimated dipole strengths at each source point, e.g., as a color map, and overlaying the map on a slice of an anatomical volume of the brain, or its surface reconstruction.

In distributed source models, it is useful to constrain the locations of the source points to the cortical gray matter and the orientations normal to the cortical mantle to improve the accuracy of the estimation (Dale et al., 2000). Application of the former constraint requires a triangulated gray matter surface and for the latter constraint, the normal vector of the cortex needs to be estimated at each vertex of the triangulation. Such detailed information about the cortex is not directly available from 3D volumetric magnetic resonance images (MRIs) of the brain. To extract this geometrical information, the cortical surface can be reconstructed from a high-resolution MR-image using a highly-automated sequential procedure (Dale et al., 1999) involving stripping of the skull, segmentation of gray and white matter volumes, separation of cortical from subcortical structures, separation of left and right hemispheres, and tessellation of

white matter and pial surfaces in each hemisphere.

Surface reconstruction is also essential for surface-based visualization, which is advantageous for several reasons. First, due to the highly folded nature of the cortical sheet, sources that are very close in a volume image may actually be far away along the surface (such as on different banks of the same sulcus). Second, visualization of activity buried in the sulci is easier if the cortex is inflated to a 2D structure. Third, if the cortex is inflated into a parametric shape (such as a sphere), then it is possible to align and average surfaces of individual subjects in order to obtain a template for group analysis. Inflation and co-registration to a sphere are performed by a sequence of steps that minimizes metric and topological distortions (Fischl et al., 1999). For surface-based analysis in this thesis work, the Free Surfer software package (http://surfer.nmr.mgh.harvard.edu, Martinos Center for Biomedical Imaging, Massachusetts General Hospital) was used.

5. Nonlinear systems identification

Systems identification is a framework originating from control theory and is concerned with the description of dynamical systems in terms of measured inputs and outputs. Since the nonlinear systems identification framework was applied in Publication I to build predictive models of induced oscillatory dynamics, this chapter describes the framework briefly. Further, the model in Publication I was inspired by the hemodynamic response function (HRF) in the analysis of fMRI signals. The main application of the HRF is to compare predicted and actual fMRI signals at each voxel and produce statistical maps of activation. Therefore, this chapter also provides a brief primer of the concepts involved in statistical parametric mapping.

5.1 Dynamical systems

The mathematical description of a dynamical system entails a set of rules (the model structure) that describes the time-behavior of the dependent variables (outputs) of a system as a function of its independent variables (inputs). For some purposes, it is convenient to express the mapping between inputs and outputs through a state space. Such models are called state-space models, or input-state-output models. The state space is spanned by state variables, which are the descriptors of the state of the dynamical system. State variables enhance the understanding of the system dynamics if they represent some physical constituents of the system. For example, in the context of cognitive neuroscience, the observable behavioral consequences of cognition (outputs) are described by mental/neural states (state variables), which in turn capture the relationship between external stimuli (inputs) and observed behavior (outputs). Hence, it is useful to think of the brain as a dynamical system.

It is useful to understand what we expect from a quantitative model of a dynamical system in general. Wu et al. (2006) offer some desirable characteristics: a good model must provide a good fit to the available data. To be practical, it must be as sparse as possible, i.e. it must explain the data based on a few key parameters. It must be computationally feasible to estimate the model parameters. To be informative, it must be biophysically meaningful, i.e. the model parameters should reflect the underlying processes. A useful model should guide experimental design by helping to test novel hypotheses about the system. Finally, a robust model should generalize well to novel patterns of input.

The approach to modeling dynamical systems may be divided into several steps. The first step is to define the set of dependent and independent variables that constitute the system. The model complexity, and consequently, the data required to estimate the model increase with the number of variables.

In the second step, prior knowledge about the system must be used to specify a suitable model structure. If the causal relationships between inputs and outputs are well known, the model structure can be specified completely from first principles. Such models are called white-box models. On the other hand, if nothing is known apriori, the model structure is minimally specified or totally unspecified, and the input–output mapping can be derived mainly from the data. These are called gray-box and black-box models, respectively.

The third step is to design and acquire a training dataset which consists of a set of input–output pairs. The design question attempts to answer what input excitations to the system maximize the amount and reliability of information extracted, from as small a number of input–output measurements as possible.

For a linear system, the design is straightforward; the system response to an excitation of arbitrary strength and infinitesimal duration is sufficient to predict the system response to an excitation of arbitrary strength and duration. However, the answer is not as straightforward for nonlinear systems. For these systems, Gaussian white-noise inputs as well as specialized sequences such as the pseudo-random m-sequence and the sum of sinusoids have been used as system inputs; these input sequences are briefly discussed by Marmarelis (1993) and authors cited therein.

The fourth step is to estimate the mapping between the inputs and

outputs, so that the output predicted by the mapping best fits the measured output. If the model is parametric, the problem reduces to the estimation of a few parameters.

The final step is to validate the model for its robustness. At the very least, it must be able to fit the training data well. It is also important to test the model on an independent test set and quantify its performance.

5.1.1 Linear time-invariant modeling

The assumptions of linearity and time invariance impose certain constraints on the relationship between the input and output of a model. In a linear system, scaling the input by a constant results in a scaling of the output by the same constant (scaling principle). In addition, the output to two or more inputs is exactly equal to the sum of outputs to individual inputs (superposition principle). Under time invariance, a time-shifted input results in exactly the same time shift in the output. Taken together, it can be shown that under the linear time-invariant assumption, the output $y(t)$ can be modeled as a convolution of an input $u(t)$ with an impulse response function (IRF) $k(t)$, defined as the system output to a vanishingly brief input $\delta(t)$ (Stremler, 1990), viz.

$$y(t) = k_0 + \int_{-\infty}^{\infty} k(\tau)u(t-\tau)\mathrm{d}\tau \tag{5.1}$$

For a causal system, $k(t) = 0$ when $t < 0$.

The validity of linearity and time-invariance can be tested using the time-shifted summation approach that evaluates whether responses to longer-duration inputs are predicted by summing shifted copies of a template response to a shorter-duration input. Typically this template is derived based on the response waveform.

5.1.2 Generalized convolution models

Linear convolution can be extended to a generalized convolution framework in which any nonlinear, time-invariant system can be expressed as an infinite series of functionals (the Volterra series) constructed by multiple convolutions of the input. For the input $u(t)$, the output $y(t)$ is given by the Volterra series as

$$
\begin{aligned}
y(t) = k_0 & \\
& + \int_{0^+}^{\infty} k_1(\tau_1) u(t-\tau_1) \mathrm{d}\tau_1 \\
& + \int \int_{0^+}^{\infty} k_2(\tau_1, \tau_2) u(t-\tau_1) u(t-\tau_2) \mathrm{d}\tau_1 \mathrm{d}\tau_2 \\
& + \int \int \ldots \int_{0^+}^{\infty} k_m(\tau_1, \tau_2, \ldots, \tau_m) u(t-\tau_1) u(t-\tau_2) \\
& \ldots u(t-\tau_m) \mathrm{d}\tau_1 \mathrm{d}\tau_2 \ldots \mathrm{d}\tau_m
\end{aligned} \tag{5.2}
$$

where k_m is called the m^{th}-order Volterra kernel. k_0 is a constant which captures the time-invariant offset. The first-order kernel k_1 represents the linear unit impulse response of the system, similar to the IRF in the linear convolution framework. Similarly, the second-order kernel k_2 is a function of two time variables and represents the system response to two unit impulses applied at different points in time. In practice, the Volterra series is often truncated to second-order because the amount of data required to estimate each higher-order kernel scales exponentially with the model order (Victor, 2005).

5.2 Model estimation

The method to estimate the linear convolution kernel from the input and output is called linear deconvolution. Deconvolution in the time domain is done by assuming that the output and input are polynomial coefficients, and then computing the quotient of the polynomials. The basis for this comes from the Z-transform (or any integral transform). If in addition to the input and output, the spectral properties of the measurement noise are known, deconvolution can also be done in the frequency domain using the Wiener filter. More general approaches to deconvolution are derived from statistical estimation theory (Kay, 1993).

If we express the linear convolution operation as a product of two matrices as $\mathbf{Y} = \mathbf{UK}$, where $\mathbf{U}$ is the input, $\mathbf{K}$ is the convolution kernel and $\mathbf{Y}$ is the output, then the kernel may be estimated by multiplying the equation by the pseudo-inverse of $\mathbf{U}$ from the left. It is well known that this minimizes the sum of squares of the residual $\mathbf{Y} - \mathbf{UK}$. However, to obtain a good estimate of $\mathbf{K}$, $\mathbf{U}$ must be non-singular in theory, and close to full-rank in practice.

The model may also be estimated in the Fourier domain. Specifi-

cally, the Fourier transform of the kernel may be estimated as the quotient of the Fourier transforms of the output and the input as

$$K(\omega) = \frac{Y(\omega)}{U(\omega)} \tag{5.3}$$

However, to ensure that $K(\omega)$ is non-zero at all frequencies, the input $u(t)$ needs to be approximately white. Regularization may be applied in the time domain (Tiknonov regularization) or the frequency domain (Wiener filter) to avoid singularities; see Kay (1993). These methods are non-parametric i.e. they do not make any assumptions about the shape of the kernel, and each time point of the kernel is estimated to best explain the input–output relationship. Linear, closed-form, non-parametric inversions are not as straightforwardly obtained for the generalized convolution model as for the linear time-invariant model.

Kernels may also be estimated by employing parametric models. In this approach, the putative shape of the kernel is approximated by a function which depends on a few parameters. Once these assumptions are made, the parameters are estimated. Such an approach significantly reduces model order compared with the non-parametric case. A sufficiently general parametric model may be developed using temporal orthogonal basis functions. The choice of the basis set depends on prior knowledge about the shape of the kernel, and the number of hyperparameters required to describe the basis set. Once this choice is made, the parameters to be estimated are simply the coefficients of the basis functions. With this approach, it is possible to relax Wiener's requirement of whiteness of input and estimate the coefficients using least-squares regression (Marmarelis, 1993).

5.3 Statistical parametric mapping

In neuroimaging studies using fMRI or PET, it is often of interest to compare brain activity in different regions across different stimuli or tasks. On the basis of imaging data, researchers seek answers to questions such as "which brain areas are statistically significantly more active during task A than during task B?". These questions can be formulated into hypotheses which can be subjected to statistical tests. Statistical parametric mapping (SPM) is a technique to perform hypothesis testing using the general linear model (GLM) (Friston, 2006). The hypothesis can be encoded in the GLM and subsequently tested. The GLM models the observed

fMRI data $\mathbf{Y}$ in terms of a linear combination of explanatory variables $\mathbf{X}$. The data can be expressed as $\mathbf{Y} = \mathbf{X}\beta + \epsilon$, where $\mathbf{X}$ consists of the explanatory variables, β are the parameters to be estimated, and ϵ is a well-behaved residual. The matrix $\mathbf{X}$ that contains the explanatory variables is called the design matrix. Each column of the design matrix corresponds to a hypothesis question or a known effect that may confound the results. These columns are referred to as explanatory variables, predictors or regressors. The parameters (weights) for each regressor, β, that best explain the data $\mathbf{Y}$, are then computed for each voxel using a least squares fit. Usually, the interesting hypotheses concern contrasts between the parameter estimates from different datasets, such as different conditions or subject groups. These parameter estimates are subjected to statistical testing to obtain measures of statistical significance in the form of a test statistic such as z scores, which can be converted to appropriate p values. Test statistics are then visualized as color maps on an anatomical brain slice or a surface rendering. These maps express the statistical certainty of observing activation in a given area. The process of visualizing maps of parametric statistics gives the technique its name.

The mathematical transformation that predicts the BOLD signal, given the pattern of stimulation or measures of neural activity, is called the HRF. The HRF is so called because it suggests that the hemodynamic activity that comes after neural activation is typically some sort of response to local energy demands. Formally, the HRF is defined as the hemodynamic response elicited by an infinitesimally short stimulus. In practice, the explanatory variables in the design matrix $\mathbf{X}$ are constructed by convolving the HRF to the signal which represents stimulus strength and duration. The HRF is known to vary across brain regions and subjects (Aguirre et al., 1998). Although a linear time-invariant model for the HRF is most commonly used, nonlinear models based on generalized convolution have also been used.

6. Independent component analysis

Independent component analysis (ICA) is one among a class of methods to achieve blind source separation. Blind source separation (BSS) is the process of recovering a set of unobserved signals from their mixtures with very little information about the underlying signals or the mixing process. It must be noted that the set of unobserved signals are referred to as sources in the BSS literature, although they have nothing to do with the current sources obtained by inverse modeling of MEG signals (see Section 4.5).

6.1 Theory

6.1.1 Statistical constraints and mixing models

All BSS methods make two types of general assumptions. First, it is necessary to assume something about the statistical properties of the sources. Second, it is necessary to adopt a generative model of the observations, i.e. a mixing model. In general, both these assumptions depend on the dataset in question.

The classical ICA method assumes (1) that the sources are non-Gaussian and mutually statistically independent, and (2) that they are mixed by a linear noiseless model. For a set of independent signals (independent components) arranged row-wise in a matrix $\mathbf{S}$, and a linear mixing matrix $\mathbf{A}$, the mixed signals $\mathbf{X}$ are given by

$$\mathbf{X} = \mathbf{AS} \tag{6.1}$$

A complex-valued equivalent of the linear mixing model has been proposed and estimated (Bingham and Hyvärinen, 2000). In addition to

classical linear mixing, noisy linear mixing, e.g. (Hyvärinen, 1999)

$$\mathbf{X} = \mathbf{AS} + n \tag{6.2}$$

and post-nonlinear mixing (Hyvärinen et al., 2001, Ch. 17)

$$\mathbf{X} = f(\mathbf{AS}) \tag{6.3}$$

are suitable alternatives for real-world data. All the above mixing models are instantaneous, i.e. they assume no delay between the observed and unobserved signals. Convolutive mixing (Hyvärinen et al., 2001, Ch. 19) is suitable to model delays in the data generative process

$$\mathbf{X} = \mathbf{A} * \mathbf{S} + n \ . \tag{6.4}$$

Fourier mixing

$$F(\mathbf{X}) = \mathbf{A}F(\mathbf{S}) \tag{6.5}$$

where $F(.)$ represents a pre-transformation to the observed data, such as a short-time Fourier transform or wavelet transform, is another alternative mixing model. The advantage of applying a pre-transformation before ICA is that under a certain class of $F(.)$ for certain types of data, the statistical properties of desirable sources are more likely to satisfy the constraints imposed by ICA. Indeed, this advantage has been exploited throughout this thesis.

6.1.2 Principles of estimation

To estimate the ICA model in Eq. 6.1, a wide range of methods have been developed. A number of these methods attempt to estimate a demixing matrix $\mathbf{W}$ by maximizing the statistical independence of the sources, so that an estimate of the sources can be subsequently obtained as $\mathbf{Y} = \mathbf{WX}$. Two popular approaches have been presented to maximize statistical independence of the sources.

The first approach involves maximizing some measure of non-Gaussianity of the sources. This approach is motivated by the central limit theorem which suggests that a maximally non-Gaussian $\mathbf{Y}$ corresponds to a maximally independent estimate of $\mathbf{S}$ (Hyvärinen et al., 2001). Typical measures of non-Gaussianity are kurtosis and negentropy.

Kurtosis is a statistical measure that captures the peakedness of the probability density, and is defined for zero-mean signals as the fourth order cumulant normalized by the square of the second order cumulant

and corrected to be zero for a Gaussian density: $\text{kurt}(s) = E(s^4)/(E(s^2))^2 - 3$. While kurtosis is an intuitive measure of non-Gaussianity, it is often not robust to outliers because it increases quickly with the number and amplitude of outliers. In particular, a few large outliers can dominate the kurtosis measure and this leads to a lack of robustness in the estimate. Kurtosis is thus more suitable for rejection of large-amplitude artifacts.

Negentropy is a measure motivated by the well-known observation that Gaussian random variables have the highest information entropy. Information entropy is defined as $H(s) = -\sum p(s)\log(p(s))$. Negentropy of a random variable s is then defined as the difference between the entropy of the signal and the entropy of a Gaussian random variable with the same variance, given by $J(s) = H(s_{\text{gauss}}) - H(s)$. In practice, negentropy is hard to estimate without knowing the probability density of the source s. However, as noted by Hyvärinen et al. (2001), various polynomial approximations of negentropy exist (Comon, 1994) and are used in practice. For instance, negentropy can be approximated as

$$\begin{aligned} J(s) &\approx k_1(E(s^3))^2 + k_2(\text{kurt}(s))^2 \\ &\approx k_1(E(s^3))^2 + k_2(E(s^4) - E(s_{\text{gauss}}^4))^2 \end{aligned} \tag{6.6}$$

where k_1 and k_2 are constants whose optimal values can be derived. If s is not skewed, the negentropy reduces to the square of the kurtosis and therefore suffers from the same lack of robustness as kurtosis. To keep the negentropy measure robust in practice, the functions s^3 and s^4 are replaced by gradually increasing nonlinear functions $G_1(s)$ and $G_2(s)$. Various choices of nonlinear functions for robust avoidance of outliers have been proposed. Of these, $G_1(s) = \log(\cosh(s))$ and $G_2(s) = -\exp(-s^2/2)$ have proven to be useful choices (Hyvärinen et al., 2001).

The second approach adopts maximum likelihood estimation by assuming a family of sparse densities for the sources S. Maximum likelihood (ML) is a classical framework in statistical estimation, in which the likelihood of observing the data under a parametric model is maximized with respect to the parameters. In practice, the log likelihood is mathematically more tractable and therefore the negative log likelihood is minimized instead (Hyvärinen et al., 2001). In the ML framework, it is possible to write down arbitrary generative models including nonlinear ones such as in Eq. 6.5 with arbitrary source probability densities $p(s)$, and estimate them with generic optimization methods. The negative log likelihood is expressed as a function of the model parameters, which in the case of ICA

are the entries of the demixing matrix. A typical approach here is to specify a parametric form of the log likelihood with a family of non-Gaussian densities $p(s)$. A Bayesian extension of the ML framework, the maximum aposteriori (MAP) framework, allows one to impose arbitrary prior information on the sources or the mixing matrix, which might be useful in situations where something is known about the statistical properties of mixing.

An alternative approach to estimate the demixing matrix W is by joint diagonalization of the covariance matrix and the higher-order cumulant tensor. One such method, joint approximate diagonalization of eigenmatrices (JADE) is based on the approximate diagonalization of the eigenmatrices of higher-order cumulant tensor of the independent components (Cardoso and Souloumiac, 1993).

In addition to methods imposing statistical independence or non-Gaussianity, temporal embedding methods such as temporal decorrelation source separation (TDSEP) (Ziehe and Müller, 1998) and second order blind identification (SOBI) (Belouchrani et al., 1997) that jointly diagonalize covariances, are also used in blind source separation. These methods are based on the constraint that for the estimated independent components, the lagged covariance matrices $C_{\tau,i,j}$, defined as $\mathrm{Cov}(s_i(t), s_j(t-\tau))$ across multiple time lags τ, must be as diagonal as possible. The rationale behind temporal embedding methods is that since instantaneous decorrelation between estimated ICs is not a sufficient condition for uniquely estimating the ICs, lagged decorrelation is imposed as an additional requirement. Lagged decorrelation is then traded for the requirement of non-Gaussianity. Thus, temporal embedding methods are capable of separating Gaussian sources.

6.1.3 Estimation techniques

A number of ICA estimation methods apply classical optimization techniques such as the natural gradient method. Gradient descent is a classical iterative method to minimize an arbitrary function. At each iteration, the parameters are perturbed in the direction of the steepest descent (negative gradient) of the function to be minimized. It has been shown that in the context of ICA, the negative natural gradient is a better estimate of the direction of steepest descent than the negative gradient itself. Hence, the natural gradient is typically used in ICA estimation. For gradient-based methods, a learning-rate parameter which specifies the amount of

perturbation at each iteration must usually be set. The main disadvantage of gradient descent based algorithms is that they converge slowly.

Fast fixed-point algorithms developed by Hyvarinen (1999) offer highly successful alternatives to gradient descent. The basic insight of these fast methods is that if w, the vector of parameters being estimated, is constrained to have unit norm (as in the case of ICA), then the gradient must point in the direction of w at each iteration. Due to the unit norm constraint, it is possible to set w equal to the gradient, and subsequently divide by its norm. This method, called FastICA, has been shown to converge an order of magnitude faster than gradient descent (Hyvarinen, 1999). FastICA has been widely used, including in publications constituting this thesis work.

6.1.4 Statistical significance

Since the majority of ICA estimation techniques are sensitive to initial conditions and susceptible to local minima, the question of how statistically repeatable the estimated components are, is an important one.

A typical strategy for achieving repeatability such as the one proposed in the ICASSO method (Himberg et al., 2004) proceeds as follows. First, the ICA estimation is repeated several times with different initial conditions or bootstrapping. Next, the resulting components are clustered using a heuristic method, and finally, only repeatable clusters (according to a heuristic measure) are retained.

In a neuroimaging (or equivalent) setting with multiple and comparable datasets, an alternative approach for establishing statistical significance selects only those components which are repeatable across subjects (or equivalent datasets) using some heuristic measure. One such realization called self-organizing ICA (sogICA), was proposed by Esposito et al. (2005), where a novel measure was used to match corresponding ICs across datasets. Recently, Hyvärinen (2011) proposed a method for testing the statistical significance of estimated independent components by assigning p values to individual components based on their similarity across subjects (datasets). By assuming that under the null hypothesis, the linear mixing matrix is a random orthogonal matrix, it was possible to derive the probability of observing an arbitrary IC, and therefore assign p values based on how unlikely the ICs were, under the null.

6.2 Applications of ICA to neuroimaging

6.2.1 Analysis of fMRI data

ICA has been widely applied to fMRI data to identify spatially independent networks. In spatial ICA (SICA) applications, the activation pattern observed at each time instant is assumed to be a mixture of spatially independent sources or networks. By contrast, in temporal ICA (TICA) applications, it is assumed that the signal at each spatial location is a mixture of temporally independent processes. Owing to their much larger spatial than temporal dimension, fMRI data have primarily been analyzed using SICA.

McKeown et al. (1998) and McKeown (2000) made some of the first attempts to analyze fMRI data with ICA. Spatial maps and IC timecourses obtained by spatial ICA were comparable to statistical parametric maps obtained by a GLM approach and the task regressors used in the design matrix of the GLM. Their results suggested that ICA is a powerful approach to analyze data in uncontrolled experiments where the stimulus or task regressors are unknown a priori.

In general, the benefit of SICA is that imposing spatial independence on the data results in spatially distinct networks that are allowed to covary temporally. Calhoun et al. (2001b) compared the application of SICA and TICA on four different experimental designs in which visual cortical networks were constrained to be either temporally dependent, spatially dependent, spatiotemporally dependent, or spatiotemporally independent. SICA was able to extract networks that were spatially independent but not necessarily networks that were temporally independent; similarly TICA was successful in extracting temporally independent networks but not spatially independent ones. The study implied that while the data-driven nature of ICA is powerful for experiments without an explicit design, the particular ICA method must be adapted to the statistical structure of the data.

To address the limitations discussed by Calhoun et al. (2001b), Stone et al. (2002) proposed skew-spatiotemporal ICA to select sources with skewed distributions. This method achieves a trade-off between exact independence in the spatial or temporal dimension alone for joint partial independence in both spatial and temporal dimensions.

6.2.2 Analysis of fMRI resting-state networks

An early application of ICA to resting-state fMRI data (Kiviniemi et al., 2003) showed that bilateral sensorimotor, visual and auditory networks could be distinctly separated from fMRI data acquired from anesthetized children. Greicius et al. (2004) showed that the default mode network could be identified with ICA in young adults, healthy elderly adults as well as Alzheimer's disease patients. Beckmann et al. (2005) and van de Ven et al. (2004) applied spatial ICA to healthy adults and reported distinctly repeatable networks viz. the medial visual network, the lateral visual network, the auditory network, the sensorimotor network, the default mode network, the dorsal visual pathways, and the executive control network, noting the hemispheric decoupling of the attention networks. The networks identified with spatial ICA were also found to have distinct spectral characteristics (van de Ven et al., 2004).

Once functionally distinct networks could be reliably identified with ICA, later investigations began to systematically explore correlations between timecourses of independent components. Functional network connectivity (FNC) by Jafri et al. (2008) is one such method to study functional connectivity between distinct networks. Using this method, significant differences in correlation between independent component timecourses were found between schizophrenia patients and healthy control subjects. ICA has also been applied to identify aberrant functional connectivity within the pain network in chronic pain patients (Malinen et al., 2010).

A primarily methodological investigation which studied the functional decomposition of resting-state data at different dimensionalities, revealed interesting insights into the potentially hierearchical organization of functional networks (Smith et al., 2009). While a smaller dimensionality (of 20) revealed the primary RSNs which have been well characterized (Beckmann et al., 2005; Damoiseaux et al., 2006), a larger dimensionality of 70 revealed a decomposition of the primary networks into highly correlated subnetworks. These studies exemplify the recent success of ICA in characterizing RSNs during health and disease.

6.2.3 Analysis of EEG/ MEG signals

Temporal ICA has successfully separated various types of artifacts from EEG/ MEG signals (Vigário, 1997). ICA has also been applied to evoked

responses to characterize their dynamic spatiotemporal generators (Makeig et al., 1999, 2002). However, applications of ICA to MEG/ EEG oscillatory activity have been more recent. Makeig et al. (2004) advocated the application of ICA to event-related oscillatory activity, assuming event-related potentials to represent time-frequency perturbations. Anemüller et al. (2003) showed that complex-valued ICA applied to spectral representation of EEG signals led to sources with a limited spectral extent and a higher degree of independence than the sources obtained by traditional ICA.

At the time of starting this thesis work, no blind source separation methods were available to characterize physiologically meaningful spontaneous oscillatory activity on the time-scale of minutes.

7. Objectives of the thesis

The goals of this thesis were to develop methods to quantify and characterize the dynamics of oscillatory activity as measured by MEG during conditions where several repeats of a short external stimulus is not available. The specific goals of the studies were:

- For Publication I, our goal was to build predictive models of the dynamics of stimulus-induced changes in oscillatory activity, so that the single-trial response to an arbitrary stimulus may be predicted from a parametric description of the stimulus design.

- For Publication II, we aimed to develop a data-driven method based on ICA to separate signals of physiological interest from sensor-level MEG recordings.

- For Publication III, we modified the method developed in Publication II to emphasize spatial and spectral sparseness and to extend the method to source–space.

- For Publication IV, (i) we sought to modify the method developed in Publication III to focus on cortico-cortical networks rather than isolated sources, (ii) we intended to extend the method to multiple subjects, and (iii) using the method developed, we aimed to study how networks identified during rest are modulated by naturalistic stimulation.

8. Summary of studies

8.1 Overview of materials and methods

8.1.1 Subjects

All data presented in this dissertation were acquired from healthy adults after written informed consent. Fourteen healthy adults (six females, eight males; mean age, 28 years; range, 22–41) took part in PI while eleven adults (six females, five males; mean age 30 years; range 23–41) took part in PII, PIII, and PIV. All recordings were approved by the Ethics Committee of the Helsinki and Uusimaa Hospital District (protocols No. 9-49/2000 and No. 95/13/03/00/2008), granted to Drs. Nina Forss and Riitta Hari.

8.1.2 Stimuli

In Publication I, tactile stimuli were delivered to the tips of the fingers of each hand, excluding the thumbs. Homologous fingers of the hands were stimulated simultaneously to engage both somatosensory cortices. For details, see Section 8.2.2. In Publication II, we employed resting-state MEG data without any stimuli delivered to the quietly resting subject. In Publication III and Publication IV, we employed naturalistic visual and auditory stimuli as well as simple tactile stimuli. The visual stimuli comprised silent movie clips showing faces, hands, or buildings, whereas the auditory stimuli comprised pure tone beeps as well as speech. For details, see Section 8.4.2.

The tactile stimuli were delivered using pneumatic diaphragms attached to the fingertips of each hand. The visual stimuli used in Publication III and Publication IV were delivered using a Vista projector (Christie

Digital Systems, Inc.) via a mirror to a back-projection screen. Auditory stimuli were generated with a piezoelectric transducer and delivered using a plastic tube. The timing of stimulus delivery was controlled using Presentation Software (version 0.81, Neurobehavioral Systems Inc., Albany, CA, USA).

8.1.3 Measurements

MEG data were acquired with a 306-channel whole-scalp MEG system (Elekta Neuromag Oy, Helsinki, Finland). Measurements for the testing dataset in PI were conducted in a two-layer shielded room equipped with active compensation. For the training dataset in PI and all data in PII–PIV, measurements were conducted in a three-layer shielded room without active compensation. The shielded rooms were located at the Brain Research Unit, O.V. Lounasmaa Laboratory, School of Science, Aalto University.

Measurements for PI were bandpass filtered to 0.03–200 Hz and digitized at 600 Hz, whereas those for PII–PIV were filtered within 0–200 Hz and digitized at 600 Hz. In addition to these measurements, a 2-min recording without a subject was conducted after each experiment to estimate the noise statistics for inverse modeling.

During the MEG recordings, four small coils, whose locations had been digitized with respect to anatomical landmarks, were briefly energized to determine the subject's head position with respect to the MEG sensors.

Anatomical MRIs were obtained using a 3-T General Electric Signa MRI scanner (Milwaukee, WI) at the Advanced Magnetic Imaging (AMI) Centre of the School of Science, Aalto University.

8.2 Modeling the amplitude dynamics of task-induced changes in MEG oscillations (PI)

8.2.1 Motivation

Induced changes in neural oscillations are time-locked but not necessarily phase-locked to the onset of a stimulus or a task. Amplitude envelopes of spontaneous oscillations are suppressed during stimulation or task performance. Most literature on the dynamics of spontaneous oscillations is

descriptive rather than predictive. To predict the suppression and subsequent rebound dynamics of task-induced oscillatory changes as a function of the task sequence, we introduced the oscillatory response function (ORF): an electrophysiological analog to the hemodynamic response function (HRF). In this study, we developed the ORF and applied it to predict the dynamics of the 20-Hz component of the rolandic mu rhythm.

8.2.2 Approach

The dynamical system which produces the suppression-rebound dynamics of the 20-Hz amplitude envelope is inherently nonlinear, since the duration and the amplitude of the rebound do not scale linearly with respect to the stimulus duration or strength. To capture such a nonlinearity, we used the generalized convolution framework. Since generalized convolution kernels capture the non-linear transformation inherent in the suppression-rebound dynamics, we preferred this framework to the linear convolution framework used to model HRFs. A Volterra series truncated to second order was used to specify the model structure for the ORF. The input of the model was a step function representing the stimulus time-course and the output was the envelope of the 20-Hz mu rhythm from a representative rolandic sensor.

To estimate the model, we expanded the kernels as a linear combination of three Laguerre basis functions and then estimated the coefficients using the Wiener method (Wiener 1958; Marmarelis 1993). Figure 8.1 shows the approach used in the model estimation. We learned the parameters of the model (i.e. the coefficients of the basis expansion) on an independent training dataset and then applied the model to predict oscillatory responses on an independent testing dataset.

For both training and testing experiments, tactile stimuli were delivered using pneumatic diaphragms at the fingertips of both hands. The stimuli for the test dataset were designed to be informative about the generalizability of the estimated model as a function of stimulus parameters. We employed a design with alternating stimulus and rest blocks and bilateral stimulation to engage the somatosensory cortex of both hemispheres. Within a stimulus block, the tactile stimuli were presented in a random order under the constraint that homologous fingers were stimulated simultaneously. The training session consisted of two 13-min sequences of pneumotactile stimulus trains. In a single train, the stimuli were given at either 4 Hz or 10 Hz. All fingers except the thumb were stimulated. Each

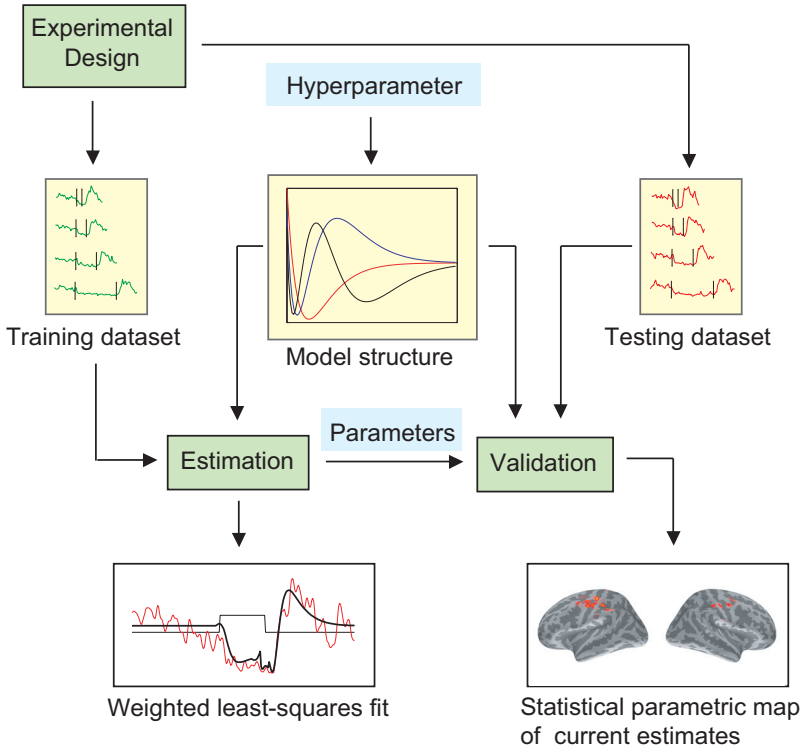

Figure 8.1. The experimental design determines the training and the testing paradigm. A suitable model structure with a hyperparameter specifies the properties of the Laguerre basis functions with a 2-s support. The training dataset is used to learn the model parameters, i.e. the coefficients of the basis functions using a weighted least squares fit. Once the parameters are estimated, they are validated on the testing dataset by computing statistical parametric maps of neuronal current estimates.

sequence consisted of 25 stimulus blocks of four different durations (0.5, 1, 2, and 4 s) occurring in a random order and the rest blocks were of five different durations (5.0, 5.5, 6.0, 6.5, and 7.0 s). The test session comprised one 11-min sequence with tactile stimuli at 4 Hz. Each stimulus sequence comprised 40 trials, each of them with a short stimulus block (1 s), a rest block (5 s), a long stimulus block (6 s), and another rest block (5 s). Only the index and middle fingers were stimulated.

8.2.3 Results and discussion

For the training dataset, the envelopes of the 20-Hz rhythms from rolandic sensors were 25–43% better predicted by the models than by the inverted stimulus timecourse (boxcar). A linear model with separate convolution kernels for onset and offset responses gave the best prediction. We studied the generalizability of this model with data from 5 different subjects dur-

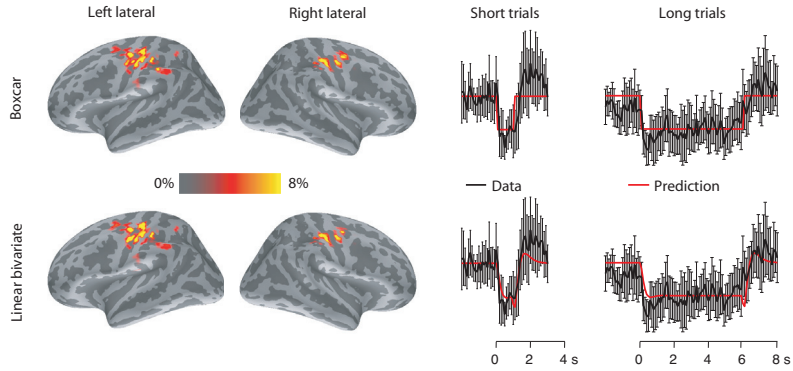

Figure 8.2. The modulation depth maps and the corresponding timecourses of the envelope for short- and long-duration trials from the maximally-modulated source point, averaged across 5 subjects, are shown. The maps are thresholded to display source points with the top 1% modulation. The timecourses are averaged across trials and subjects. Error bars show standard errors of mean. The data are shown in black and the model predictions are shown in red.

ing a separate bilateral tactile sequence by first projecting the sensor-level activity in the ~20-Hz frequency range into source space using cortically constrained minimum norm estimates. Both the model and the boxcar predicted strongest modulation in the primary motor cortex. Figure 8.2 shows maps of modulation depth estimated by the boxcar and the ORF model as predictors of the amplitude envelope. For short-duration stimulus blocks, the model predicted the envelope of the cortical currents 20% better than the boxcar did. These results suggest that ORFs could concisely describe brain rhythms during different stimuli, tasks, and pathologies. Thus, we advocate the framework as a broad, quantitative approach to characterize oscillatory dynamics of brain rhythms with specific temporal, spectral, and spatial characteristics.

8.3 Sparse time-frequency objects in sensor space: A superior method to conventional temporal ICA (PII)

8.3.1 Motivation

ICA has successfully identified resting-state networks from fMRI data. Owing to the large number of independent spatial observations in fMRI data, spatial ICA is more common. However, temporal ICA is more commonly applied to EEG/ MEG data. Prior to this publication, temporal ICA had mostly been successful in separating and removing artifacts from

recordings over time-scales of minutes, see e.g., Vigário (1997). Thus, one desirable property of a new method is that it must be successful at separating physiologically meaningful sources. Secondly, among the large number of independent components obtained, an objective method of ranking them would be useful. Finally, to describe functional connectivity within spatially-extended neural sources with possible phase delays, it would be useful to obtain the extended source in one single component. In this study, we proposed a new method called temporal Fourier-ICA with the above desirable properties and compared it against existing blind source separation methods using simulated as well as real resting-state MEG data.

8.3.2 Approach

It is well known in the theory of blind source separation that ICA maximizes sparseness along whichever data dimension it is applied. Given that artifacts in MEG data tend to be temporally sparse, it follows that temporal ICA succeeds in isolating these artifacts well. By comparison, neurophysiological sources tend to be amplitude-modulated (AM) narrowband oscillations and not necessarily sparse in the time domain. An improved data representation in which the neurophysiological sources are sparse would lead to better separation performance. As opposed to the time domain, AM narrowband oscillations are sparser in the frequency domain than artifacts.

We first explicitly demonstrated this phenomenon using simulations. Next, we proposed a linear complex-valued mixing model of complex-valued time-frequency atoms represented as short time Fourier transform coefficients. To estimate this model, we adopted an objective function that is a robust measure of non-Gaussianity and subsequently applied complex-valued FastICA (Bingham and Hyvärinen, 2000). We called the method temporal Fourier-ICA (TFICA). Using simulated as well as real MEG resting-state data, we compared Fourier-ICA against real-valued FastICA with a tanh objective function, real-valued FastICA with a kurtotic measure of non-Gaussianity, JADE (Cardoso and Souloumiac, 1993) on the time-frequency representation, SOBI (Belouchrani et al., 1997) with real-valued mixing. For FastICA, we included a reliability analysis using ICASSO framework (Himberg et al., 2004), and a threshold reliability index of 0.75 was used.

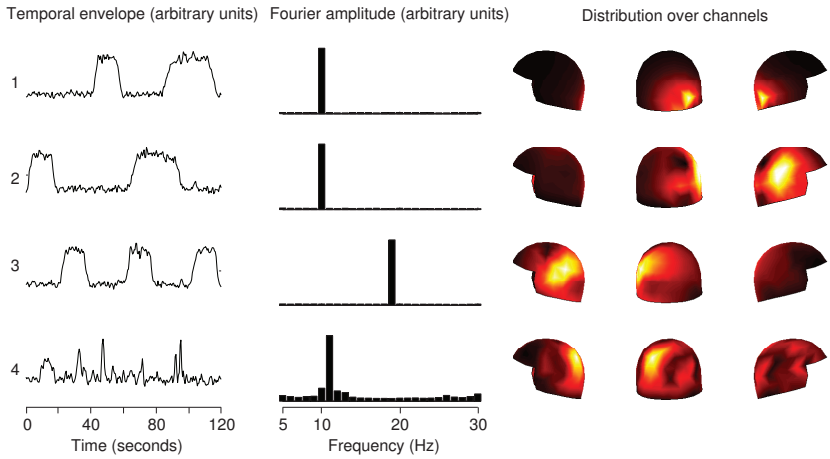

Figure 8.3. Simulated data: The first three out of four reliable sources estimated using Fourier-ICA correspond to the underlying sources in the simulation. First column: temporal envelope, second column: Fourier amplitudes, third column: power distribution over channels of 4 reliable independent components obtained using Fourier-ICA. Taken from PII with permission.

8.3.3 Results and discussion

From a simulated dataset comprising three artifactual sources and three AM sources, multiple repeats of Fourier-ICA extracted AM sources 77% of the time compared with temporal ICA which found these sources 17% of the time. Figure 8.3 shows the four reliable sources estimated from a simulation with three AM current dipoles placed in the right occipital, right Rolandic and the left Rolandic regions, mixed with real measurements from MEG sensors in the absence of a subject. The simulated sources were ranked from 1–3. By comparison, temporal ICA with tanh nonlinearity found only one simulated source, while temporal ICA with the kurtotic objective function did not find any reliable source. SOBI found 2 out of 3 sources, while JADE found all 3 sources. Figure 8.4 shows the reliable components obtained using Fourier-ICA from a real 5-min resting-state dataset from a single subject.

To conclude, our new method was able to successfully identify several narrow-band oscillatory neural sources, automatically identify the spatial, temporal and spectral structure, and provide an automatic way of ranking them in order of interestingness. These results suggest that a sparse representation of the data and a rich signal model which captures the oscillatory time structure is likely to be better at separating sources of neurophysiological interest.

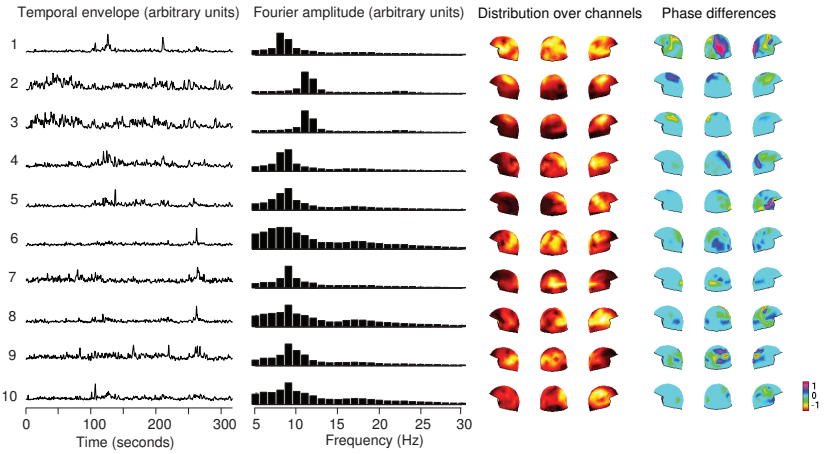

Figure 8.4. Real MEG recording: reliable sources obtained by Fourier-ICA with a complex mixing matrix. Each row is one source; the sources are ordered by the objective function, i.e. the most "interesting" ones at the top. First column: the timecourse of the source (envelope). Second column: the Fourier amplitude spectrum. Third column: the magnitudes of the sources at the topographic sensor helmet. Fourth column: the phase differences of the sources. Cyan indicates zero phase difference. Taken from PII with permission.

8.4 Maximizing spatial and spectral sparseness of Fourier coefficients in cortical space (PIII)

8.4.1 Motivation

In this study, we pursued several logical extensions of the method developed in PII. First, we extended Fourier-ICA to the cortical level by combining a distributed source localization method with a blind source separation method. Second, we exploited the observation that the three-way data (i.e. observations along spatial, temporal and spectral dimensions) are spatially sparse by imposing sparseness in the spatial and spectral dimension rather than the temporal and spectral dimensions (PII). We named this method spatial Fourier-ICA (SFICA). Third, we compared SFICA using simulations and real MEG data acquired during naturalistic stimulation to conventional spatial ICA. Finally, we applied the resulting method, spatial Fourier-ICA, to resting-state and naturalistic stimulation to the individual MEG data acquired from 9 subjects.

8.4.2 Approach

The stimuli used in the experiment were modified from Malinen et al. (2007) and comprised auditory (tone beeps, speech), visual (videos of faces,

hands or buildings), and tactile stimuli (pneumatic pulses to homologous fingers) in blocks of 6–33 s. The auditory stimuli comprised blocks of 0.1-s pure tone beeps at discrete frequencies between 250–4000 Hz presented at 5 Hz within a block, as well as blocks of a male voice narrating the history of the university or guitar instructions. The experiment consisted of three parts: (i) natstim (2×8-min; auditory, visual and tactile blocks without any rest periods in between) (ii) nat&rest (2×12 min; similar to natstim but the stimulus blocks were interspersed with 15-s rest blocks), and (iii) restfix (2×10 min; quiet rest, eyes open, fixating on a crosshair).

Figure 8.5 shows the analysis streams for the two methods. For SFICA, we projected the short time Fourier transforms of the MEG data to the cortical surface using minimum-norm estimation, , i.e., by multiplication with the linear inverse operator matrix $\mathbf{G}$. We then rearranged the three-way data by concatenating the Fourier coefficients source point by source point such that each row constitutes the Fourier coefficients over space, and each column is a time window.

8.4.3 Results and discussion

Figure 8.6 shows an independent component from a single subject obtained with SFICA, representing the consistently found ~10-Hz occipital alpha rhythm. SFICA was applied by temporal concatenation of the spatio-spectral data representation across the two natstim, restfix and nat&rest runs. The ~10- and ~20-Hz Rolandic mu rhythms were also consistently found across subjects. Figure 8.7 shows the manually selected alpha and the mu rhythm components averaged across 8 subjects. A clear suppression to visual and tactile stimuli, respectively, were seen.

Thus, SFICA enables inference about oscillatory activity under different conditions at the cortical level, and across different subject groups, such as patients and healthy volunteers over time scales of minutes. By interrogating the component timecourses (Fourier power) one can study e.g., functional connectivity between different components of the same subject, modulation of oscillatory activity by naturalistic stimuli, and repeatability of activity timecourses, within and across subjects.

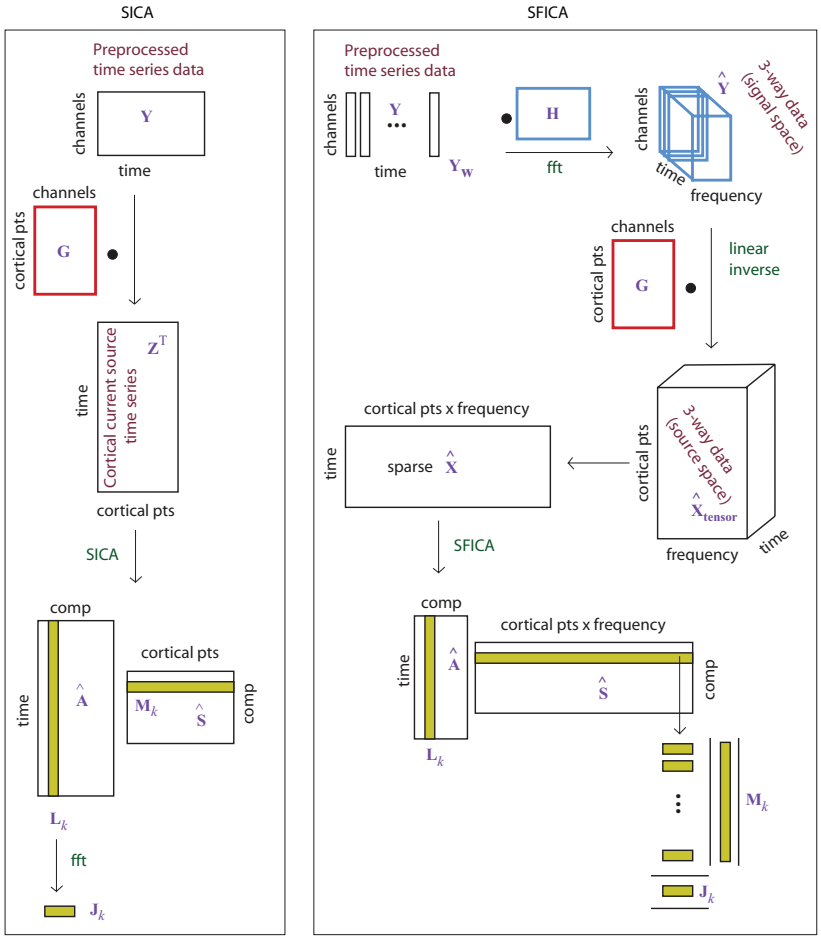

Figure 8.5. Illustration of the steps involved in the spatial ICA (left) and spatial Fourier-ICA (right) methods. Taken with permission from PIII.

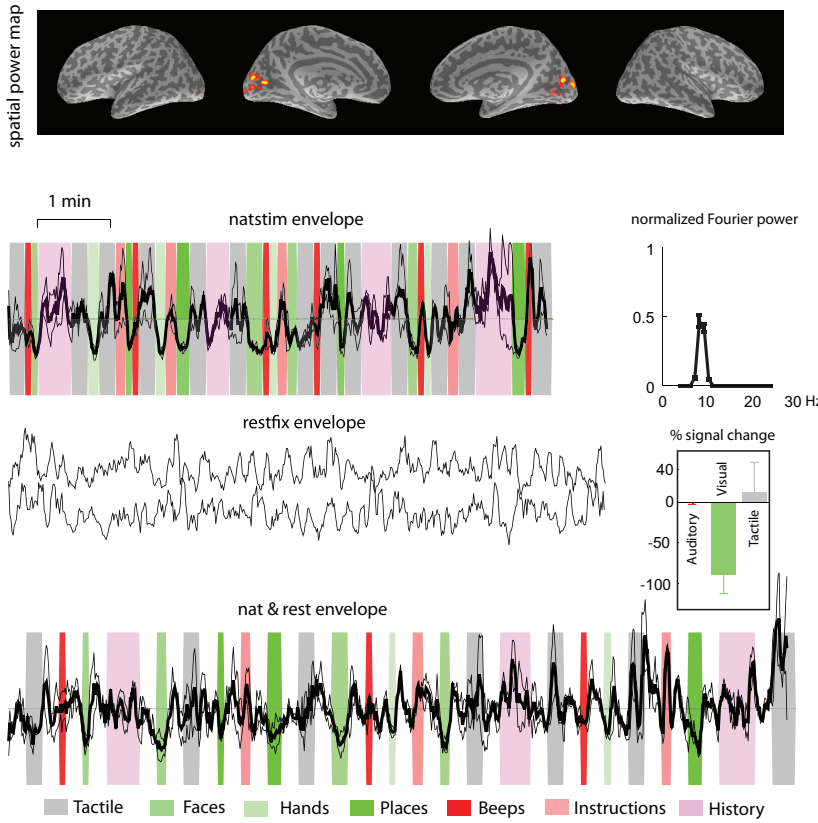

Figure 8.6. One independent component estimated using SFICA, representing the ~10-Hz occipital alpha rhythm from a single subject. The spatial power maps, thresholded to show the surface points with top 5% strength, are overlaid on the inflated brain surfaces of that subject. The timecourses show the z-scores of the envelopes overlaid for the two runs of each condition. The background represents the stimulus sequence: green bands represent visual stimuli, red bands represent auditory stimuli, and gray bands represent tactile stimuli. The natstim and nat&rest conditions show a clear suppression to all three categories of visual stimuli. Taken with permission from PIII.

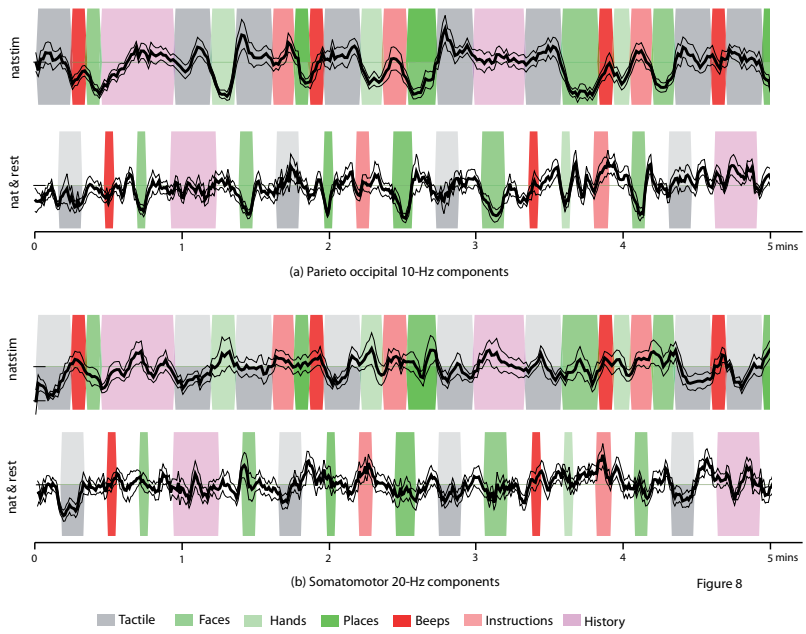

Figure 8.7. Envelopes of ~10-Hz occipital components (above) and ~20-Hz Rolandic components (below) averaged across eight subjects; the components (one per subject) were selected manually by visual inspection for each subject. Clear suppression is observed during visual (above) and tactile (below) stimulation. Taken with permission from PIII.

8.5 Group-level spatial ICA of Fourier power: How are resting-state networks modulated during naturalistic stimulation? (PIV)

8.5.1 Motivation

The Fourier-based methods developed in PII and PIII automatically extract narrowband oscillations from broadband data without having to manually specify a frequency band of interest. Whereas the methods successfully found physiologically meaningful components such as alpha and mu rhythms, they were typically located to a single cortical region. In PIV, we investigated how to robustly characterize electrophysiological resting-state networks using Fourier-based methods. In addition, we studied how MEG resting-state oscillatory networks are modulated by stimulation.

8.5.2 Approach

We hypothesized that the resting-state connectivity across brain regions is manifest in the correlations between envelopes of oscillations. Accordingly, we applied real-valued TFICA or SFICA on the broadband Fourier spectra (magnitudes of the Fourier coefficients) rather than complex-valued ICA on the complex-valued Fourier coefficients. We call these methods envelope SFICA (eSFICA) or envelope TFICA (eTFICA). After benchmarking these envelope methods against the other ICA-based variants using a realistic simulated dataset, we applied group-level eSFICA to 10-min resting-state data concatenated across 9 healthy subjects (see Section 8.4.1), separately for two runs. We then selected 30 consistent components that were most similar across the two runs using a statistical testing method (Hyvärinen, 2011). Each independent component estimated with eSFICA can be considered as a linear "spatiospectral" filter, which describes the cortical distribution of an oscillatory network. We applied these filters to 12-min short-time Fourier transforms of naturalistic stimulation data from the same 9 subjects and extracted the envelope time-courses of each resting-state network. We then examined these envelopes for modulation to external stimulation.

8.5.3 Results and discussion

We manually grouped the obtained resting-state components into approximate categories such as sensorimotor, medial visual, lateral visual, audi-

tory, higher-order sensorimotor, intrinsic, and orbitofrontal components. The method identified several networks which resemble previously reported resting-state networks, such as the bilateral sensorimotor network at ~20 Hz, the lateral and medial parieto-occipital sources at ~10 Hz, a subset of the default-mode network at ~8 and ~15 Hz, and lateralized temporal lobe sources at ~8 Hz. We observed occipital alpha modulation to visual stimuli, bilateral rolandic mu modulation to tactile stimuli and video clips of hands, and the temporal lobe network modulation to speech stimuli, but no modulation of the sources in the default-mode network. Figure 8.8 shows the spatial and spectral profiles of the sensorimotor and visual independent components obtained from resting-state data, and the modulation of the envelope dynamics of these components during naturalistic stimulation.

Our method characterized resting-state oscillatory brain networks at the cortical level across subjects. The identified RSNs were in agreement with those previously reported in the fMRI and MEG literature. Further, we showed that a majority of these RSNs were consistently modulated by external stimulation, while the intrinsic networks remained seemingly unaffected by stimulation. Since eSFICA operates on the Fourier amplitudes rather than complex-valued spectra, the captured interactions are envelope correlations and they disregard phase interactions. Further, since the ICs are zero-mean, it is possible to find envelope anti-correlations using this method. Compared with the method applied by Brookes et al. (2011), our method is automatically able to select relevant narrow frequency bands in a data-driven manner. As a result, the method can potentially find cross-frequency interactions within a single network. However, unlike Brookes et al. (2011), we did not find the classical default mode network or dorsal attention network with eSFICA.

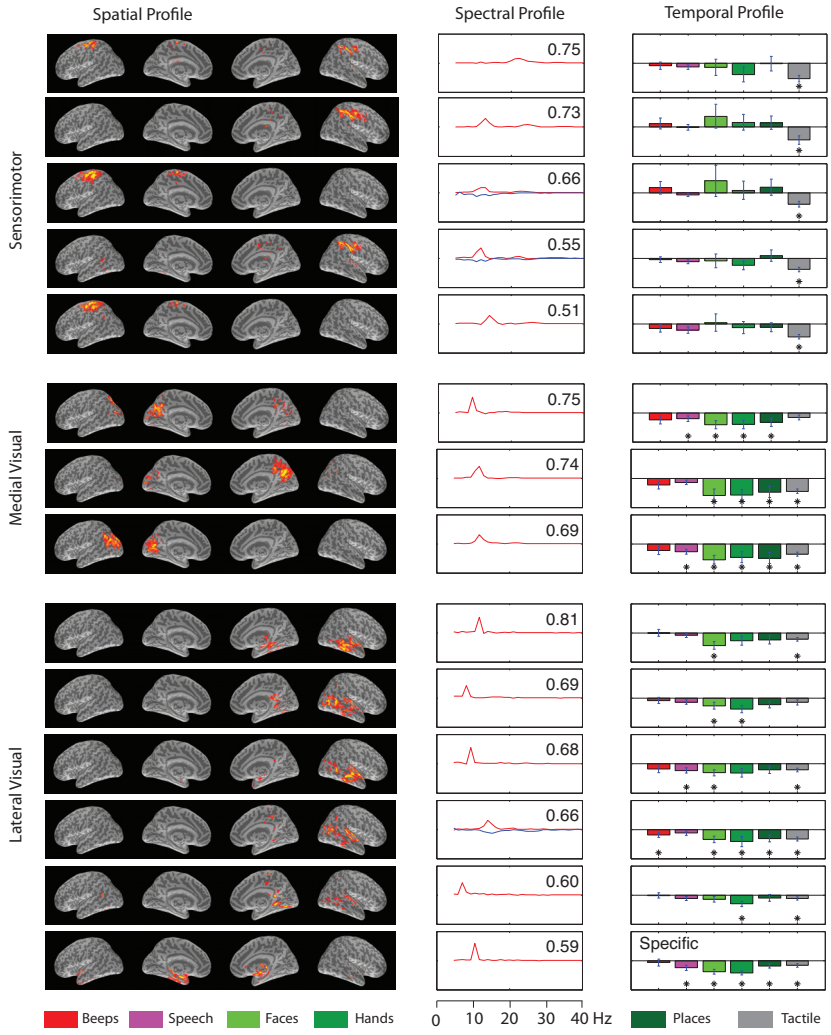

Figure 8.8. eSFICA spatiospectral filters obtained from resting-state data (left and middle panels) used to interrogate brain dynamics during natural stimulation (right panel). We manually ordered the components according to the dominant modality as sensorimotor, medial visual and lateral visual components. The inset shows consistency of the spatiospectral filter across two resting-state sessions as measured by Pearson's correlation coefficient. The temporal profile is described by the modulation depths for each stimulus category averaged across subjects. Adapted from PIV.

9. General discussion

9.1 Contributions of the thesis

This thesis presents important methodological contributions to enable predictive modeling of event-related induced oscillatory dynamics. In particular, a generalized convolution framework for learning the shape of the amplitude modulation of an oscillatory response is proposed. The learned response shape can then be used to predict the response to novel stimuli or tasks. The parametric description of the learned response also enables parsimonious comparison of event-related amplitude modulations across conditions and subjects. The framework is very general in the sense that it does not depend on the specific physiological oscillation being studied.

The thesis also develops methods for data-driven characterization of spatial, spectral and temporal aspects of spontaneous oscillatory activity over timescales of minutes. Using time-frequency representation, distributed inverse modeling, and a blind source separation method as ingredients, several variants of the method including spatial vs. temporal, sensor-level vs. cortical-level, and complex-valued short-time Fourier representation vs. real-valued short-time Fourier envelope representation, were developed and tested on simulated and real resting-state and naturalistic stimulation MEG data.

9.2 Limitations of the thesis

9.2.1 Methodological considerations

Although we proposed a ranking scheme for the estimated independent components in Publication II in terms of the objective function, it does not provide a complete answer to a practioner of the method for a principled choice of the number of independent components to estimate. In particular, the number of degrees of freedom in the data is determined by several technical factors including the degree of independence between the sensors, the number of basis functions used to represent the signal by the SSS method, the conductor model in the forward solution, the density of cortical sampling used in the distributed inverse model, as well as the underlying hierarchical organization of functional oscillatory networks. More rigorous empirical work and simulation-based research is needed to understand the relationships between these factors.

To perform inter-subject analysis, we followed the most popular approach in Publication IV based on temporal concatenation (Calhoun et al., 2001a). Temporal concatenation is an elegant solution to the inter-subject consistency problem, but it assumes that the components are present in a majority of the subjects analyzed. Further, the extent to which a component is consistently present across subjects is hard to quantify.

9.2.2 Theoretical limitations

Although we developed a predictive model of the dynamics of mu rhythm using a very general framework, the lack of a biophysically realistic ORF model does not give us any insight in the functional role of oscillations or the mechanisms that may subserve their event-related dynamics. In future work, biophysically realistic models such as those by Jones et al. (2009) or Jansen and Rit (1995) could be integrated into the predictive framework.

9.3 Suggestions for future work

To avoid the assumptions and caveats of temporal concatenation, a few alternative methods for group analysis have been proposed in the literature. Esposito et al. (2005) proposed to apply ICA on single subjects fol-

lowed by clustering of components using a heuristic measure of correspondence. Hyvärinen (2011) proposed a statistical test for the significance of an independent component based on the null hypothesis of a random orthogonal mixing matrix. Such principled methods to assess inter-subject or inter-session consistency would be an important step for the future.

Independent component analysis assumes a linear mixture of underlying sources of networks. Although this may be a valid assumption for slow temporal fluctuations observed with fMRI, more sophisticated nonlinear mixing models or dependent component models which take into account the empirically-observed cross-frequency phase synchrony or phase-amplitude coupling (van der Meij et al., 2012) could be more effective. For instance, evidence from intracranial recordings and MEG signals suggests that oscillations at different frequencies are related in a hierarchical nested manner, where the phase of low frequencies are correlated with the ampltude of high frequencies (Canolty et al., 2006). BSS methods with a hierarchical observation model could be useful to express the hierarchical nature of nested oscillations.

In the future, to understand the neural basis of BOLD resting-state networks, it would be extremely crucial to seek evidence from complementary functional imaging methods, such as intracranial recordings. New data showing phase-amplitude coupling (van der Meij et al., 2012) as well as the emergence of persistent networks (Kramer et al., 2011) in intracranial recordings are promising in this context.

Finally, although we have deployed naturalistic stimuli in our studies, we have not made any computational characterization of the particular stimuli. To bring the knowledge gained from classical experiments with artificial stimuli to bear upon exploratory analysis of brain responses to naturalistic stimuli, computational generative models which explain how naturalistic stimuli, such as scenes or faces, are built from elementary constituents such as oriented edges and textures would be extremely valuable. Multimodal studies combining behavioral measurements such as eye-tracking with neural activity measurements would be particularly valuable in this regard.

Bibliography

Aguirre, G., Zarahn, E., D'Esposito, M., 1998. The variability of human, BOLD hemodynamic responses. Neuroimage 8 (4), 360–369.

Ahonen, A. I., Hämäläinen, M. S., Kajola, M. J., Knuutila, J. E. T., Laine, P. P., Lounasmaa, O. V., Parkkonen, L. T., Simola, J. T., Tesche, C. D., 1993. 122-channel squid instrument for investigating the magnetic signals from the human brain. Physica Scripta T49A, 198–205.

Andrews-Hanna, J. R., Snyder, A. Z., Vincent, J. L., Lustig, C., Head, D., Raichle, M. E., Buckner, R. L., 2007. Disruption of large-scale brain systems in advanced aging. Neuron 56 (5), 924–935.

Anemüller, J., Sejnowski, T. J., Makeig, S., 2003. Complex independent component analysis of frequency-domain electroencephalographic data. Neural Networks 16 (9), 1311–1323.

Baker, S., Gabriel, C., Lemon, R., 2003. EEG oscillations at 600 hz are macroscopic markers for cortical spike bursts. Journal of Physiology 550 (2), 529–534.

Bartels, A., Zeki, S., 2004. Functional brain mapping during free viewing of natural scenes. Human Brain Mapping 21 (2), 75–85.

Beckmann, C. F., DeLuca, M., Devlin, J. T., Smith, S. M., 2005. Investigations into resting-state connectivity using independent component analysis. Philosophical Transactions of the Royal Society B: Biological Sciences 360 (1457), 1001 –1013.

Belouchrani, A., Abed-Meraim, K., Cardoso, J. F., Moulines, E., 1997. A blind source separation technique using second-order statistics. IEEE Transactions on Signal Processing 45 (2), 434–444.

Bingham, E., Hyvärinen, A., 2000. A fast fixed-point algorithm for independent component analysis of complex valued signals. International Journal of Neural Systems 10 (1), 1–8.

Biswal, B., Zerrin Yetkin, F., Haughton, V. M., Hyde, J. S., 1995. Functional connectivity in the motor cortex of resting human brain using echo-planar MRI. Magnetic Resonance in Medicine 34 (4), 537–541.

Bressler, S. L., Kelso, J., 2001. Cortical coordination dynamics and cognition. Trends in Cognitive Sciences 5 (1), 26–36.

Brookes, M. J., Woolrich, M., Luckhoo, H., Price, D., Hale, J. R., Stephenson, M. C., Barnes, G. R., Smith, S. M., Morris, P. G., 2011. Investigating the electrophysiological basis of resting state networks using magnetoencephalography. Proceedings of the National Academy of Sciences USA 108 (40), 16783–16788.

Buckner, R. L., Snyder, A. Z., Shannon, B. J., LaRossa, G., Sachs, R., Fotenos, A. F., Sheline, Y. I., Klunk, W. E., Mathis, C. A., Morris, J. C., Mintun, M. A., 2005. Molecular, structural, and functional characterization of Alzheimer's disease: Evidence for a relationship between default activity, amyloid, and memory. Journal of Neuroscience 25 (34), 7709–7717.

Buehlmann, A., Deco, G., 2010. Optimal information transfer in the cortex through synchronization. PLoS Computational Biology 6 (9), e1000934.

Caetano, G., Jousmäki, V., Hari, R., 2007. Actor's and observer's primary motor cortices stabilize similarly after seen or heard motor actions. Proceedings of the National Academy of Sciences USA 104 (21), 9058–9062.

Calhoun, V. D., Adali, T., Pearlson, G. D., Pekar, J. J., 2001a. A method for making group inferences from functional MRI data using independent component analysis. Human Brain Mapping 14 (3), 140–151.

Calhoun, V. D., Adali, T., Pearlson, G. D., Pekar, J. J., May 2001b. Spatial and temporal independent component analysis of functional MRI data containing a pair of task-related waveforms. Human Brain Mapping 13 (1), 43–53.

Canolty, R. T., Edwards, E., Dalal, S. S., Soltani, M., Nagarajan, S. S., Kirsch, H. E., Berger, M. S., Barbaro, N. M., Knight, R. T., 2006. High gamma power is phase-locked to theta oscillations in human neocortex. Science 313 (5793), 1626 –1628.

Cardoso, J. F., Souloumiac, A., 1993. Blind beamforming for non-Gaussian signals. Radar and Signal Processing, IEE Proceedings F 140 (6), 362–370.

Cohen, D., 1968. Magnetoencephalography: Evidence of magnetic fields produced by alpha-rhythm currents. Science 161 (3843), 784 –786.

Cohen, D., 1972. Magnetoencephalography: Detection of the brain's electrical activity with a superconducting magnetometer. Science 175 (4022), 664 –666.

Cohen, D., Schlapfer, U., Ahlfors, S., Hämäläinen, M., Halgren, E., 2002. New six-layer magnetically-shielded room for MEG. In: 13th International Conference on Biomagnetism. VDE Verlag, Jena, Germany.

Comon, P., 1994. Independent component analysis, a new concept? Signal Processing 36 (3), 287–314.

Dale, A., Liu, A., Fischl, B., R.L., B., Belliveau, J., Lewine, J., Halgren, E., 2000. Dynamic statistical parametric mapping: Combining fMRI and MEG for high-resolution imaging of cortical activity. Neuron 26 (1), 55–67.

Dale, A. M., Fischl, B., Sereno, M. I., 1999. Cortical surface-based analysis: I. segmentation and surface reconstruction. NeuroImage 9 (2), 179–194.

Dale, A. M., Sereno, M. I., 1993. Improved localizadon of cortical activity by combining EEG and MEG with MRI cortical surface reconstruction: A linear approach. Journal of Cognitive Neuroscience 5 (2), 162–176.

Damoiseaux, J. S., Rombouts, S. a. R. B., Barkhof, F., Scheltens, P., Stam, C. J., Smith, S. M., Beckmann, C. F., 2006. Consistent resting-state networks across healthy subjects. Proceedings of the National Academy of Sciences USA 103 (37), 13848–13853.

David, O., Friston, K. J., 2003. A neural mass model for MEG/EEG:: coupling and neuronal dynamics. NeuroImage 20 (3), 1743–1755.

de Pasquale, F., Della Penna, S., Snyder, A. Z., Lewis, C., Mantini, D., Marzetti, L., Belardinelli, P., Ciancetta, L., Pizzella, V., Romani, G. L., Corbetta, M., 2010. Temporal dynamics of spontaneous MEG activity in brain networks. Proceedings of the National Academy of Sciences USA.

Deco, G., Jirsa, V., McIntosh, A. R., Sporns, O., Kötter, R., 2009. Key role of coupling, delay, and noise in resting brain fluctuations. Proceedings of the National Academy of Sciences USA 106 (25), 10302 –10307.

Epstein, R., Kanwisher, N., 1998. A cortical representation of the local visual environment. Nature 392 (6676), 598–601.

Ermentrout, G., Chow, C. C., 2002. Modeling neural oscillations. Physiology & Behavior 77 (4–5), 629–633.

Esposito, F., Scarabino, T., Hyvarinen, A., Himberg, J., Formisano, E., Comani, S., Tedeschi, G., Goebel, R., Seifritz, E., Di Salle, F., 2005. Independent component analysis of fMRI group studies by self-organizing clustering. NeuroImage 25 (1), 193–205.

Fair, D. A., Cohen, A. L., Dosenbach, N. U. F., Church, J. A., Miezin, F. M., Barch, D. M., Raichle, M. E., Petersen, S. E., Schlaggar, B. L., 2008. The maturing architecture of the brain's default network. Proceedings of the National Academy of Sciences USA 105 (10), 4028–4032.

Felsen, G., Dan, Y., 2005. A natural approach to studying vision. Nature Neuroscience 8 (12), 1643–1646.

Fischl, B., Sereno, M. I., Dale, A. M., 1999. Cortical Surface-Based analysis: II: inflation, flattening, and a Surface-Based coordinate system. NeuroImage 9 (2), 195–207.

Fox, M. D., Raichle, M. E., 2007. Spontaneous fluctuations in brain activity observed with functional magnetic resonance imaging. Nature Reviews Neuroscience 8 (9), 700–711.

Fox, M. D., Snyder, A. Z., Vincent, J. L., Corbetta, M., Van Essen, D. C., Raichle, M. E., 2005. The human brain is intrinsically organized into dynamic, anticorrelated functional networks. Proceedings of the National Academy of Sciences USA 102 (27), 9673–9678.

Fries, P., 2005. A mechanism for cognitive dynamics: neuronal communication through neuronal coherence. Trends in Cognitive Sciences 9 (10), 474–480.

Fries, P., 2009. Neuronal gamma-band synchronization as a fundamental process in cortical computation. Annual Review of Neuroscience 32 (1), 209–224.

Friston, K., 2006. Statistical Parametric Mapping: The Analysis of Functional Brain Images., 1st Edition. Elsevier Science and Technology, Amsterdam, The Netherlands.

Gastaut, H., 1952. Electrocorticographic study of the reactivity of rolandic rhythm. Revue Neurologique 87 (2), 176–182.

Giraud, A., Kleinschmidt, A., Poeppel, D., Lund, T. E., Frackowiak, R. S., Laufs, H., 2007. Endogenous cortical rhythms determine cerebral specialization for speech perception and production. Neuron 56 (6), 1127–1134.

Goldman, R. I., Stern, J. M., Engel, J., Cohen, M. S., 2002. Simultaneous EEG and fMRI of the alpha rhythm. NeuroReport 13 (18), 2487–2492.

Golland, Y., Bentin, S., Gelbard, H., Benjamini, Y., Heller, R., Nir, Y., Hasson, U., Malach, R., 2007. Extrinsic and intrinsic systems in the posterior cortex of the human brain revealed during natural sensory stimulation. Cerebral Cortex 17 (4), 766–777.

Granger, C., 1969. Investigating causal relations by econometric models and cross-spectral methods. Econometrica 37 (3), 424–438.

Greicius, M., 2008. Resting-state functional connectivity in neuropsychiatric disorders. Current Opinion in Neurology 24 (4), 424–430.

Greicius, M. D., 2003. Functional connectivity in the resting brain: A network analysis of the default mode hypothesis. Proceedings of the National Academy of Sciences USA 100 (1), 253–258.

Greicius, M. D., Kiviniemi, V., Tervonen, O., Vainionpää, V., Alahuhta, S., Reiss, A. L., Menon, V., 2008. Persistent default-mode network connectivity during light sedation. Human Brain Mapping 29 (7), 839–847.

Greicius, M. D., Srivastava, G., Reiss, A. L., Menon, V., 2004. Default-mode network activity distinguishes alzheimer's disease from healthy aging: Evidence from functional MRI. Proceedings of the National Academy of Sciences USA 101 (13), 4637–4642.

Gross, J., Kujala, J., Hämäläinen, M., Timmermann, L., Schnitzler, A., Salmelin, R., 2001. Dynamic imaging of coherent sources: Studying neural interactions in the human brain. Proceedings of the National Academy of Sciences USA 98 (2), 694–699.

Hari, R., 1990. Magnetic evoked fields of the human brain: basic principles and applications. Electroencephalography and Clinical Neurophysiology. Supplement 41, 3–12.

Hari, R., 2004. Magnetoencephalography in clinical neurophysiological assessment of human cortical functions. In: Niedermeyer, E., Da Silva, F. (Eds.), Electroencephalography: Basic Principles, Clinical Applications, and Related Fields. Lippincott Williams & Wilkins, pp. 1165–1197.

Hari, R., Forss, N., Avikainen, S., Kirveskari, E., Salenius, S., Rizzolatti, G., 1998. Activation of human primary motor cortex during action observation: A neuromagnetic study. Proceedings of the National Academy of Sciences USA 95 (25), 15061 –15065.

Hari, R., Salmelin, R., 1997. Human cortical oscillations: a neuromagnetic view through the skull. Trends in Neurosciences 20 (1), 44–49.

Hari, R., Salmelin, R., 2012. Magnetoencephalography: From SQUIDs to neuroscience. Neuroimage EPub Ahead of Print.

Hasson, U., Furman, O., Clark, D., Dudai, Y., Davachi, L., 2008a. Enhanced intersubject correlations during movie viewing correlate with successful episodic encoding. Neuron 57 (3), 452–462.

Hasson, U., Nir, Y., Levy, I., Fuhrmann, G., Malach, R., 2004. Intersubject synchronization of cortical activity during natural vision. Science 303 (5664), 1634 –1640.

Hasson, U., Yang, E., Vallines, I., Heeger, D. J., Rubin, N., 2008b. A hierarchy of temporal receptive windows in human cortex. Journal of Neuroscience 28 (10), 2539–2550.

Haxby, J., Ungerleider, L., Horwitz, B., Maisog, J., Rapoport, S., Grady, C., 1996. Face encoding and recognition in the human brain. Proceedings of the National Academy of Sciences USA 93 (2), 922.

He, B. J., Snyder, A. Z., Zempel, J. M., Smyth, M. D., Raichle, M. E., 2008. Electrophysiological correlates of the brain's intrinsic large-scale functional architecture. Proceedings of the National Academy of Sciences USA 105 (41), 16039 –16044.

Himberg, J., Hyvärinen, A., Esposito, F., 2004. Validating the independent components of neuroimaging time series via clustering and visualization. NeuroImage 22 (3), 1214–1222.

Honey, C. J., Sporns, O., Cammoun, L., Gigandet, X., Thiran, J. P., Meuli, R., Hagmann, P., 2009. Predicting human resting-state functional connectivity from structural connectivity. Proceedings of the National Academy of Sciences USA 106 (6), 2035 –2040.

Hoogenboom, N., Schoffelen, J., Oostenveld, R., Parkes, L. M., Fries, P., 2006. Localizing human visual gamma-band activity in frequency, time and space. NeuroImage 29 (3), 764–773.

Hubel, D. H., Wiesel, T. N., 1963. Shape and arrangement of columns in cat's striate cortex. Journal of Physiology 165 (3), 559–568.2.

Hyvarinen, A., 1999. Fast and robust fixed-point algorithms for independent component analysis. IEEE Transactions on Neural Networks 10, 626–634.

Hyvärinen, A., 1999. Gaussian moments for noisy independent component analysis. IEEE Signal Processing Letters 6 (6), 145–147.

Hyvärinen, A., 2011. Testing the ICA mixing matrix based on inter-subject or inter-session consistency. NeuroImage 58 (1), 122–136.

Hyvärinen, A., Karhunen, J., Oja, E., Jun. 2001. Independent component analysis. John Wiley and Sons.

Hämäläinen, M., Hari, R., Ilmoniemi, R. J., Knuutila, J., Lounasmaa, O. V., 1993. Magnetoencephalography—theory, instrumentation, and applications to noninvasive studies of the working human brain. Reviews of Modern Physics 65 (2), 413–497.

Hämäläinen, M. S., Ilmoniemi, R. J., 1994. Interpreting magnetic fields of the brain: minimum norm estimates. Medical & Biological Engineering & Computing 32 (1), 35–42.

Ioannides, A. A., Bolton, J. P. R., Clarke, C. J. S., 1990. Continuous probabilistic solutions to the biomagnetic inverse problem. Inverse Problems 6 (4), 523–542.

Jafri, M. J., Pearlson, G. D., Stevens, M., Calhoun, V. D., 2008. A method for functional network connectivity among spatially independent resting-state components in schizophrenia. NeuroImage 39 (4), 1666–1681.

Jansen, B. H., Rit, V. G., 1995. Electroencephalogram and visual evoked potential generation in a mathematical model of coupled cortical columns. Biological Cybernetics 73 (4), 357–366.

Jensen, O., Gelfand, J., Kounios, J., Lisman, J. E., 2002. Oscillations in the alpha band (9–12 Hz) increase with memory load during retention in a short-term memory task. Cerebral Cortex 12 (8), 877–882.

Jones, S. R., Pritchett, D. L., Sikora, M. A., Stufflebeam, S. M., Hämäläinen, M., Moore, C. I., 2009. Quantitative analysis and biophysically realistic neural modeling of the MEG mu rhythm: Rhythmogenesis and modulation of sensory-evoked responses. Journal of Neurophysiology 102 (6), 3554–3572.

Kanwisher, N., McDermott, J., Chun, M. M., 1997. The fusiform face area: A module in human extrastriate cortex specialized for face perception. Journal of Neuroscience 17 (11), 4302 –4311.

Kay, S. M., 1993. Fundamentals of Statistical Signal Processing, Volume I: Estimation Theory, 1st Edition. Prentice Hall.

Kiviniemi, V., Kantola, J., Jauhiainen, J., Hyvärinen, A., Tervonen, O., 2003. Independent component analysis of nondeterministic fMRI signal sources. NeuroImage 19 (2), 253–260.

Klimesch, W., 1996. Memory processes, brain oscillations and EEG synchronization. International Journal of Psychophysiology 24 (1–2), 61–100.

Kramer, M. A., Eden, U. T., Lepage, K. Q., Kolaczyk, E. D., Bianchi, M. T., Cash, S. S., 2011. Emergence of persistent networks in long-term intracranial EEG recordings. Journal of Neuroscience 31 (44), 15757–15767.

Kujala, J., Vartiainen, J., Laaksonen, H., Salmelin, R., 2012. Neural interactions at the core of phonological and semantic priming of written words. Cerebral Cortex EPub Ahead of Print.

Larson-Prior, L. J., Zempel, J. M., Nolan, T. S., Prior, F. W., Snyder, A. Z., Raichle, M. E., 2009. Cortical network functional connectivity in the descent to sleep. Proceedings of the National Academy of Sciences USA 106 (11), 4489–4494.

Laufs, H., Krakow, K., Sterzer, P., Eger, E., Beyerle, A., Salek-Haddadi, A., Kleinschmidt, A., 2003. Electroencephalographic signatures of attentional and cognitive default modes in spontaneous brain activity fluctuations at rest. Proceedings of the National Academy of Sciences USA 100 (19), 11053–11058.

Lehongre, K., Ramus, F., Villiermet, N., Schwartz, D., Giraud, A., 2011. Altered Low-Gamma sampling in auditory cortex accounts for the three main facets of dyslexia. Neuron 72 (6), 1080–1090.

Leopold, D. A., Murayama, Y., Logothetis, N. K., 2003. Very slow activity fluctuations in monkey visual cortex: Implications for functional brain imaging. Cerebral Cortex 13 (4), 422–433.

Lin, F., Witzel, T., Ahlfors, S., Stufflebeam, S., Belliveau, J., Hämäläinen, M., 2006. Assessing and improving the spatial accuracy in meg source localization by depth-weighted minimum-norm estimates. Neuroimage 31 (1), 160–171.

Logothetis, N. K., Pauls, J., Augath, M., Trinath, T., Oeltermann, A., 2001. Neurophysiological investigation of the basis of the fMRI signal. Nature 412 (6843), 150–157.

Lopes da Silva, F. H., Hoeks, A., Smits, H., Zetterberg, L. H., 1974. Model of brain rhythmic activity. Kybernetik 15 (1), 27–37.

Lu, H., Zuo, Y., Gu, H., Waltz, J. A., Zhan, W., Scholl, C. A., Rea, W., Yang, Y., Stein, E. A., 2007. Synchronized delta oscillations correlate with the resting-state functional MRI signal. Proceedings of the National Academy of Sciences USA 104 (46), 18265–18269.

Magri, C., Schridde, U., Murayama, Y., Panzeri, S., Logothetis, N., 2012. The amplitude and timing of the BOLD signal reflects the relationship between local field potential power at different frequencies. Journal of Neuroscience 32 (4), 1395–1407.

Makeig, S., Debener, S., Onton, J., Delorme, A., 2004. Mining event-related brain dynamics. Trends in Cognitive Sciences 8 (5), 204–210.

Makeig, S., Westerfield, M., Jung, T., Covington, J., Townsend, J., Sejnowski, T. J., Courchesne, E., 1999. Functionally independent components of the late positive Event-Related potential during visual spatial attention. Journal of Neuroscience 19 (7), 2665–2680.

Makeig, S., Westerfield, M., Jung, T., Enghoff, S., Townsend, J., Courchesne, E., Sejnowski, T. J., 2002. Dynamic brain sources of visual evoked responses. Science 295 (5555), 690–694.

Malinen, S., Hlushchuk, Y., Hari, R., 2007. Towards natural stimulation in fMRI—Issues of data analysis. NeuroImage 35 (1), 131–139.

Malinen, S., Vartiainen, N., Hlushchuk, Y., Koskinen, M., Ramkumar, P., Forss, N., Kalso, E., Hari, R., 2010. Aberrant temporal and spatial brain activity during rest in patients with chronic pain. Proceedings of the National Academy of Sciences USA 107 (4), 6493–6497.

Mallet, N., Pogosyan, A., Sharott, A., Csicsvari, J., Bolam, J. P., Brown, P., Magill, P. J., 2008. Disrupted dopamine transmission and the emergence of exaggerated beta oscillations in subthalamic nucleus and cerebral cortex. Journal of Neuroscience 28 (18), 4795–4806.

Mantini, D., Perrucci, M. G., Del Gratta, C., Romani, G. L., Corbetta, M., 2007. Electrophysiological signatures of resting state networks in the human brain. Proceedings of the National Academy of Sciences USA 104 (32), 13170 –13175.

Marmarelis, P. Z., McCann, G. D., 1973. Development and application of white-noise modeling techniques for studies of insect visual nervous system. Kybernetik 12 (2), 74–89.

Marmarelis, V. Z., 1993. Identification of nonlinear biological systems using laguerre expansions of kernels. Annals of Biomedical Engineering 21 (6), 573–589.

Mason, M. F., Norton, M. I., Van Horn, J. D., Wegner, D. M., Grafton, S. T., Macrae, C. N., 2007. Wandering minds: The default network and stimulus-independent thought. Science 315 (5810), 393–395.

McKeown, M. J., 2000. Detection of consistently task-related activations in fMRI data with hybrid independent component analysis. NeuroImage 11 (1), 24–35.

McKeown, M. J., Makeig, S., Brown, G., Jung, T., Kindermann, S., Bell, A., Sejnowski, T., 1998. Analysis of fMRI data by blind separation into independent spatial components. Human Brain Mapping 6 (3), 160–188.

Moosmann, M., Ritter, P., Krastel, I., Brink, A., Thees, S., Blankenburg, F., Taskin, B., Obrig, H., Villringer, A., 2003. Correlates of alpha rhythm in functional magnetic resonance imaging and near infrared spectroscopy. NeuroImage 20 (1), 145–158.

Mäkelä, J. P., Kirveskari, E., Seppä, M., Hämäläinen, M., Forss, N., Avikainen, S., Salonen, O., Salenius, S., Kovala, T., Randell, T., Jääskeläinen, J., Hari, R., 2001. Three-dimensional integration of brain anatomy and function to facilitate intraoperative navigation around the sensorimotor strip. Human Brain Mapping 12 (3), 180–192.

Nenonen, J., Kajola, J., Simola, A., Ahonen, A., 2004. Total information of multichannel meg sensor arrays. In: 14th Int. Conf. on Biomagnetism, E. Halgren, S. Ahlfors, M. Hämäläinen, and D. Cohen, eds. Biomag2004 Ltd, Boston, 2004, pp. 630–631.

Niedermeyer, E., Da Silva, F., 2005. Electroencephalography: Basic Principles, Clinical Applications, and Related Fields. Lippincott Williams & Wilkins.

Nir, Y., Mukamel, R., Dinstein, I., Privman, E., Harel, M., Fisch, L., Gelbard-Sagiv, H., Kipervasser, S., Andelman, F., Neufeld, M. Y., Kramer, U., Arieli, A., Fried, I., Malach, R., 2008. Interhemispheric correlations of slow spontaneous neuronal fluctuations revealed in human sensory cortex. Nature Neuroscience 11 (9), 1100–1108.

Okada, Y. C., Wu, J., Kyuhou, S., 1997. Genesis of MEG signals in a mammalian CNS structure. Electroencephalography and Clinical Neurophysiology 103 (4), 474–485.

Palva, J. M., Palva, S., Kaila, K., 2005a. Phase synchrony among neuronal oscillations in the human cortex. Journal of Neuroscience 25 (15), 3962–3972.

Palva, S., Linkenkaer-Hansen, K., Näätänen, R., Palva, J. M., May 2005b. Early neural correlates of conscious somatosensory perception. Journal of Neuroscience 25 (21), 5248–5258.

Palva, S., Palva, J. M., 2007. New vistas for alpha-frequency band oscillations. Trends in Neurosciences 30 (4), 150–158.

Papanicolaou, A., Simos, P., Castillo, E., Breier, J., Sarkari, S., Pataraia, E., Billingsley, R., Buchanan, S., Wheless, J., Maggio, V., et al., 2004. Magnetocephalography: a noninvasive alternative to the wada procedure. Journal of Neurosurgery 100, 867–876.

Pascual-Marqui, R., Michel, C., Lehmann, D., 1994. Low resolution electromagnetic tomography: a new method for localizing electrical activity in the brain. International Journal of Psychophysiology 18 (1), 49–65.

Pikovsky, A., Rosenblum, M., 2007. Synchronization. Scholarpedia 2 (12), 1459. URL http://www.scholarpedia.org/article/Synchronization

Quiroga, R. Q., Reddy, L., Kreiman, G., Koch, C., Fried, I., 2005. Invariant visual representation by single neurons in the human brain. Nature 435 (7045), 1102–1107.

Raichle, M. E., Mintun, M. A., 2006. Brain work and brain imaging. Annual Review of Neuroscience 29, 449–476.

Salmelin, R., Hari, R., 1994. Spatiotemporal characteristics of sensorimotor neuromagnetic rhythms related to thumb movement. Neuroscience 60 (2), 537–550.

Salmelin, R., Hámáaláinen, M., Kajola, M., Hari, R., 1995. Functional segregation of movement-related rhythmic activity in the human brain. Neuroimage 2 (4), 237–243.

Sasaki, K., Tsujimoto, T., Nambu, A., Matsuzaki, R., Kyuhou, S., 1994. Dynamic activities of the frontal association cortex in calculating and thinking. Neuroscience Research 19 (2), 229–233.

Schnitzler, A., Salenius, S., Salmelin, R., Jousmäki, V., Hari, R., 1997. Involvement of primary motor cortex in motor imagery: A neuromagnetic study. NeuroImage 6 (3), 201–208.

Shulman, G. L., Fiez, J. A., Corbetta, M., Buckner, R. L., Miezin, F. M., Raichle, M. E., Petersen, S. E., 1997. Common blood flow changes across visual tasks: II. Decreases in cerebral cortex. Journal of Cognitive Neuroscience 9 (5), 648–663.

Simões, C., Jensen, O., Parkkonen, L., Hari, R., 2003. Phase locking between human primary and secondary somatosensory cortices. Proceedings of the National Academy of Sciences USA 100 (5), 2691–2694.

Smith, S. M., Fox, P. T., Miller, K. L., Glahn, D. C., Fox, P. M., Mackay, C. E., Filippini, N., Watkins, K. E., Toro, R., Laird, A. R., Beckmann, C. F., 2009. Correspondence of the brain's functional architecture during activation and rest. Proceedings of the National Academy of Sciences USA 106 (31), 13040–13045.

Stefan, H., Hummel, C., Scheler, G., Genow, A., Druschky, K., Tilz, C., Kaltenhäuser, M., Hopfengärtner, R., Buchfelder, M., Romstöck, J., 2003. Magnetic brain source imaging of focal epileptic activity: a synopsis of 455 cases. Brain 126, 2396–2405.

Stone, J., Porrill, J., Porter, N., Wilkinson, I., 2002. Spatiotemporal independent component analysis of event-related fMRI data using skewed probability density functions. NeuroImage 15 (2), 407–421.

Stremler, F. G., 1990. Introduction to Communication Systems, 3rd Edition. Prentice Hall.

Tanzer, I. O., 2006. Numerical modeling in electro- and magnetoencephalography. Ph.D. thesis, Helsinki University of Technology.

Taulu, S., Kajola, M., 2005. Presentation of electromagnetic multichannel data: The signal space separation method. Journal of Applied Physics 97 (12), 124905–124910.

Taulu, S., Simola, J., 2006. Spatiotemporal signal space separation method for rejecting nearby interference in MEG measurements. Physics in Medicine and Biology 51 (7), 1759–1768.

Tiihonen, J., Hari, R., Kajola, M., Karhu, J., Ahlfors, S., Tissari, S., 1991. Magnetoencephalographic 10-Hz rhythm from the human auditory cortex. Neuroscience Letters 129 (2), 303–305.

Tiihonen, J., Kajola, M., Hari, R., 1989. Magnetic mu rhythm in man. Neuroscience 32 (3), 793–800.

Uhlhaas, P. J., Haenschel, C., Nikolić, D., Singer, W., 2008. The role of oscillations and synchrony in cortical networks and their putative relevance for the pathophysiology of schizophrenia. Schizophrenia Bulletin 34 (5), 927 –943.

Uusitalo, M., Ilmoniemi, R., 1997. Signal-space projection method for separating MEG or EEG into components. Medical and Biological Engineering and Computing 35, 135–140.

Uutela, K., Hämäläinen, M., Somersalo, E., 1999. Visualization of magnetoencephalographic data using minimum current estimates. NeuroImage 10 (2), 173–180.

van de Ven, V., Formisano, E., Prvulovic, D., Roeder, C., Linden, D., 2004. Functional connectivity as revealed by spatial independent component analysis of fmri measurements during rest. Human Brain Mapping 22 (3), 165–178.

van der Meij, R., Kahana, M., Maris, E., 2012. Phase–amplitude coupling in human electrocorticography is spatially distributed and phase diverse. Journal of Neuroscience 32 (1), 111–123.

Vanhatalo, S., Palva, J., Holmes, M., Miller, J., Voipio, J., Kaila, K., 2004. Infraslow oscillations modulate excitability and interictal epileptic activity in the human cortex during sleep. Proceedings of the National Academy of Sciences USA 101 (14), 5053–5057.

Victor, J. D., 2005. Analyzing receptive fields, classification images and functional images: challenges with opportunities for synergy. Nat Neurosci 8 (12), 1651–1656.

Vigário, R. N., 1997. Extraction of ocular artefacts from EEG using independent component analysis. Electroencephalography and Clinical Neurophysiology 103 (3), 395–404.

Wu, M. C., David, S. V., Gallant, J. L., 2006. Complete functional characterization of sensory neurons by system identification. Annual Review of Neuroscience 29 (1), 477–505.

Ziegler, D., Pritchett, D., Hosseini-Varnamkhasti, P., Corkin, S., Hämäläinen, M., Moore, C., Jones, S., 2010. Transformations in oscillatory activity and evoked responses in primary somatosensory cortex in middle age: a combined computational neural modeling and MEG study. Neuroimage 52, 897–912.

Ziehe, A., Müller, K., 1998. TDSEP — an efficient algorithm for blind separation using time structure. In: International Conference on Artificial Neural Networks (ICANN '98). pp. 675–680.

Zimmerman, J. E., Thiene, P., Harding, J. T., 1970. Design and operation of stable rf-biased superconducting point-contact quantum devices, and a note on the properties of perfectly clean metal contacts. Journal of Applied Physics 41 (4), 1572–1580.

Aalto-DD 56/2012

ISBN 978-952-60-4615-0
ISBN 978-952-60-4616-7 (pdf)
ISSN-L 1799-4934
ISSN 1799-4934
ISSN 1799-4942 (pdf)

Aalto University
School of Science
Brain Research Unit, O.V. Lounasmaa Laboratory
www.aalto.fi

BUSINESS +
ECONOMY

ART +
DESIGN +
ARCHITECTURE

SCIENCE +
TECHNOLOGY

CROSSOVER

**DOCTORAL
DISSERTATIONS**